Health State Estimation and Remaining Useful Life Prediction of Power Devices Subject to Noisy and Aperiodic Condition Monitoring

Zhao, Shuai; Peng, Yingzhou; Yang, Fei; Ugur, Enes; Akin, Bilal; Wang, Huai

Published in:
IEEE Transactions on Instrumentation and Measurement

DOI (link to publication from Publisher):
10.1109/TIM.2021.3054429

Publication date:
2021

Document Version
Accepted author manuscript, peer reviewed version

This article has been accepted for publication in a future issue of this journal, but has not been fully edited. Content may change prior to final publication. Citation information: DOI 10.1109/TIM.2021.3054429, IEEE Transactions on Instrumentation and Measurement

Health State Estimation and Remaining Useful Life Prediction of Power Devices Subject to Noisy and Aperiodic Condition Monitoring

Shuai Zhao, *Member, IEEE*, Yingzhou Peng, *Member, IEEE*, Fei Yang, *Student Member, IEEE*, Enes Ugur, *Member, IEEE*, Bilal Akin, *Senior Member, IEEE*, and Huai Wang, *Senior Member, IEEE*

***Abstract*—Condition monitoring of power devices is highly critical for safety and mission critical power electronics systems. Typically, these systems are subjected to noise in harsh operational environment contaminating the degradation measurements. In dynamic applications, the system duty cycle may not be periodic and result in aperiodic degradation measurements. Both of these factors negatively affect the health assessment performance. In order to address these challenges, this paper proposes a health state estimation and remaining useful life prediction method for power devices in the presence of noisy and aperiodic degradation measurements. For this purpose, three-source uncertainties in the degradation modeling, including the temporal uncertainty, measurement uncertainty, and device-to-device heterogeneity, are formulated in a Gamma state-space model to ensure health assessment accuracy. In order to learn the device degradation behavior, a model parameter estimation method is developed based on a stochastic expectation-maximization algorithm. The accuracy and robustness of the proposed method are verified by numerical analysis under various noise levels. Finally, the findings are justified using SiC MOSFETs accelerated aging test data.**

***Index Terms*—Degradation modeling, Gamma process, noisy and aperiodic measurements, SiC MOSFETs, particle filter, RUL prediction.**

NOMENCLATURE

$x(t)$	Health state of a power device at time t.
t	Condition monitoring time.
$\nu(t)$	Time-varying shape parameter of $x(t)$.
u	Scale parameter of $x(t)$.
$\Gamma(\cdot)$	Gamma function.
$y(t)$	Degradation measurements.
ε	Measurement noise.
σ^2	Variance of measurement noise ε.
$B(\cdot,\cdot)$	Beta function.
ξ	Reciprocal form of scale parameter u.
κ	Shape parameter of ξ.
λ	Reciprocal form of the scale parameter of ξ.
$\mathcal{F}_{\cdot,\cdot}$	$\mathcal{F}$ distribution.
x_F	Predefined critical level.
T_F	Failure time.
t_R	Remaining useful life.
$\boldsymbol{\Theta}$	Model parameter set.
i	Index of the power device.
m	Number of power devices.
j	Index of condition monitoring time instant.
$t_{i,j}$	jth condition monitoring time instant of ith device.
n_i	Number of monitoring time instants of ith device.
$L(\cdot)$	Likelihood function.
N	Number of particles (or smoothers).
$\bar{x}_{i,0}^{(d)a}$	Augmented mean of dth particle.
$P^{(d)a}$	Augmented covariance matrix.
$\chi_{j-1}^{(d)a}$	Sigma points of dth particle at time t_{j-1}.
K_j	Kalman gain at time t_j.
w	Weights of particles (or smoothers).

Shuai Zhao, Yingzhou Peng, and Huai Wang are with the Department of Energy Technology, Aalborg University, Aalborg 9220, Denmark. (Email: szh@et.aau.dk; ype@et.aau.dk; hwa@et.aau.dk)

Fei Yang, Enes Ugur, and Bilal Akin are with the Department of Electrical and Computer Science, University of Texas at Dallas, Richardson, TX 75080 USA (Email: fei.yang1@utdallas.edu; enesugur@gmail.com; bilal.akin@utdallas.edu).

I. INTRODUCTION

RECENTLY, condition monitoring (CM) [1], health state estimation, and remaining useful life (RUL) [2]–[5] of critical power devices have been receiving a growing interest to mitigate catastrophic risks of power electronic systems. The continuously accumulated CM data lay a solid foundation for data-driven methods for RUL prediction. In power electronics field, various data-driven methods have been proposed, e.g., statistical regression-based method [4], [6], neural network [5], Bayesian filter [7], principal component analysis (PCA) [8], Gaussian process regression [9], [10], etc. As for data-driven methods, the signal quality and features are essential for accurate and robust RUL prediction. Nevertheless, due to high sensitivity requirements in CM tools and harsh operational environment (e.g., electromagnetic inference), degradation measurement signals applied for RUL prediction are subjected to contamination by a large amount of noise [2], [11], [12]. It is a well-known fact that the device health state deteriorates continuously throughout the system lifetime [2], [13], [14]. If such noisy degradation measurements are directly applied to RUL prediction, the health assessment results become misleading and trigger false alarms especially for the fixed-threshold systems [14], [15]. It is a long-lasting challenge in the field of power electronics to develop accurate, robust, and cost-effective condition monitoring methods.

In the presence of noisy degradation measurements, typically one type of method is used to reduce the noise at the data preprocessing stage. Generally, smoothing techniques are performed on degradation measurements to generate a fitted sequence. For example, in [11], a symmetrical low-pass filter is applied to eliminate the noise in the degradation

measurement $V_{\mathrm{CE(on)}}$ of insulated-gate bipolar transistors (IGBTs). Then, the filtered $V_{\mathrm{CE(on)}}$ is input into the degradation modeling stage based on a Markov stochastic duration model. In [2], a signal outlier removal driven by a random sample consensus algorithm is applied to the increment of drain-to-source on-state resistance $\Delta R_{\mathrm{DS(on)}}$ of power metal-oxide field-effect transistors (MOSFETs) to improve the accuracy of RUL prediction. In [16], the measurement $\Delta R_{\mathrm{DS(on)}}$ of power MOSFETs is filtered by computing the mean of constitutive data points to suppress the noise in the RUL prediction. Although such noise elimination methods may work well in some cases, the details of CM signals are excessively omitted without considering the underlying degradation characteristics (e.g., monotonic degradation trend), which may lead to low evaluation accuracy and counterintuitive results [14], [15].

Another way dealing with noisy degradation measurements is state-space model [7], [16]–[20]. Compared to the smoothing techniques, the state-space model can proactively and directly exploit the noise degradation measurements rather than eliminating the noise. This model considers the noisy degradation measurements as the external observations, based on which it will recursively estimate the internal health states for the degradation modeling and RUL prediction. The model framework is flexible and can provide superior RUL prediction in various engineering applications, e.g., Lithium-ion battery [18], [20], light-emitting diodes [19], milling machine [21], etc. However, most existing state-space models are not applicable to the condition monitoring of power devices due to the following three reasons. Firstly, the power devices continuously deteriorate and hence the corresponding health state changes of devices are considered as monotonic [14]. In most cases, this inherent monotonic feature has not been adequately considered. Secondly, during the monitoring, CM system duty cycle may not be periodic or several scheduled equidistant CM procedures may fail randomly, which results in aperiodic CM sequences [21]. As such, the existing state-space models (e.g., [18]–[20]) for RUL prediction, are difficult to apply due to the underlying model assumption of the fixed CM time interval. Thirdly, uncertainty sources, which are critical for RUL prediction tasks [22], [23], have been rarely considered comprehensively in the field of power electronics. These uncertainties include three aspects from the temporal uncertainty, measurement uncertainty, and device-to-device heterogeneity [22]. Temporal uncertainty refers to inherent uncertainty in operation conditions resulting in the time-varying statistical characteristics (e.g., coefficient of variation) in degradation measurements [24]. It can be handled by using stochastic processes, e.g., Gamma process, Wiener process, etc. Measurement uncertainty refers to degradation measurements that are contaminated with noise and disturbance, making the actual device health state hidden. To address this issue, a state-space model structure can be applied to eliminate the noise effect iteratively for estimating the health state [22]. The third uncertainty is caused by the device-to-device heterogeneity, which is due to the device material properties and manufacturing tolerances. Even if the power devices are from the same batch, each device possesses a unique degradation pattern and the device population may have high-level heterogeneity. It can be handled by using a device-specific random effect in model parameters, which should be considered in degradation model to maintain the accuracy of RUL prediction [22], [25]–[27].

Motivated by the above concerns, this paper proposes a health state estimation and RUL prediction method of power devices subjected to a noisy and aperiodic CM scheme. A framework based on a Gamma state-space model is proposed to track the implicit monotonic health state changes for accurate RUL prediction of power devices. This framework is developed by extending the ones in [15], [28] to further consider the three-source uncertainties together in RUL prediction. The contributions of this paper include

1) A Gamma state-space model is proposed to tackle the noisy and aperiodic degradation measurements in condition monitoring applications of power devices. The noisy and aperiodic degradation measurements can be directly used for RUL prediction. The features of the monotonic health state changes and aperiodic CM can be ensured theoretically with the proposed method.
2) Three-source uncertainties, including temporal uncertainty, measurement uncertainty, and device-to-device heterogeneity, are simultaneously incorporated in degradation model for more accurate health assessment.
3) As an exemplary application, the proposed method is implemented on the condition monitoring of SiC MOSFETs. The proposed method is generic and can be extended to other critical power devices, components, and converters.

The rest of the paper is organized as follows. Section II presents a Gamma state-space model for the degradation modeling of power devices. In Section III, the model parameter estimation method is developed and verified by a numerical study. To illustrate industrial potentials, Section IV presents a practical case study on the degradation data of SiC MOSFETs from an accelerated testing experiment. Finally, conclusions are summarized in Section V.

II. Degradation Modeling of Power Devices

In a harsh operational environment, the degradation measurements are noisy and fluctuating, masking the deteriorating behavior of power devices. It is the combination of the underlying health state and instrumental measurement errors. The degradation measurement can be considered as indirect information, which is somehow related to the internal monotonic health state change of power devices. As such, the task of health state estimation can be formulated as a stochastic filtering problem where the inherent monotonic change of health state of power device needs to be optimally estimated based on noisy and aperiodic degradation measurements. Fig. 1 presents a flowchart of the proposed method. It consists of three parts, including data collection, degradation behavior learning, and health assessment. The data collection part records the original noisy and aperiodic measurements from a batch of devices. In the degradation behavior learning part, the model is established and characterized based on the estimated monotonic health state paths. This model can be applied to

This article has been accepted for publication in a future issue of this journal, but has not been fully edited. Content may change prior to final publication. Citation information: DOI 10.1109/TIM.2021.3054429, IEEE Transactions on Instrumentation and Measurement

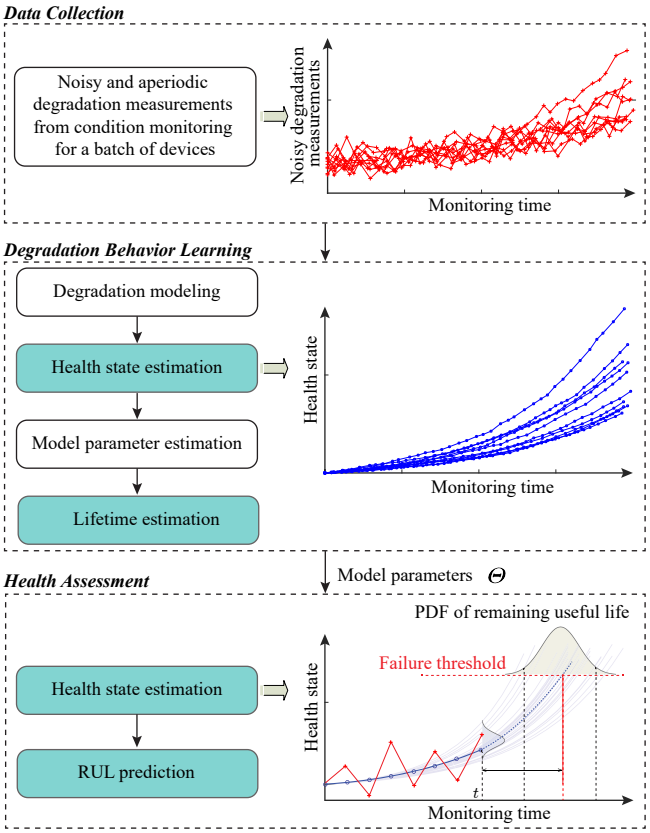

Fig. 1. Flowchart of the proposed framework for condition monitoring of power devices with noisy and aperiodic degradation measurements. The green blocks are essential functions.

the lifetime estimation of a batch of devices. In the health assessment part, the health state can be recursively estimated from the noisy and aperiodic measurements for the RUL prediction of a specific device in service.

Considering the positive increment property of Gamma process [29]–[31], the monotonic degradation behavior of power devices can be essentially fulfilled by applying a Gamma process to characterize the health state changes. Suppose that the health state path $x(t)$ is driven by a non-homogeneous Gamma process. The probability density function (PDF) of $x(t)$ can be expressed as

$$f(x;\nu,u)=\frac{1}{u\Gamma(\nu(t))}(\frac{x}{u})^{\nu(t)-1}\exp(-\frac{x}{u}),x>0, \quad (1)$$

where the non-decreasing and right-continuous function $\nu(t)>0$ denotes the shape parameter, $u>0$ is the scale parameter, and $\Gamma(\cdot)$ is the Gamma function. According to the properties of Gamma process, the degradation model possesses two main properties [30]: 1) For any CM time instants $0\le t_1<t_2<\cdots<\infty$, the health state increments, i.e., $\Delta x(0,t_1)$, $\Delta x(t_1,t_2)$, $\cdots$, are mutually independent random variables; and 2) Given any CM time intervals $[t_1,t_2]$, the corresponding increment $\Delta x(t_1,t_2)$ is a Gamma distributed variable with the mean $[\nu(t_2)-\nu(t_1)]u$ and the variance $[\nu(t_2)-\nu(t_1)]u^2$.

For a stochastic filtering task, the health state transition model in the Gamma state-space framework is formulated as

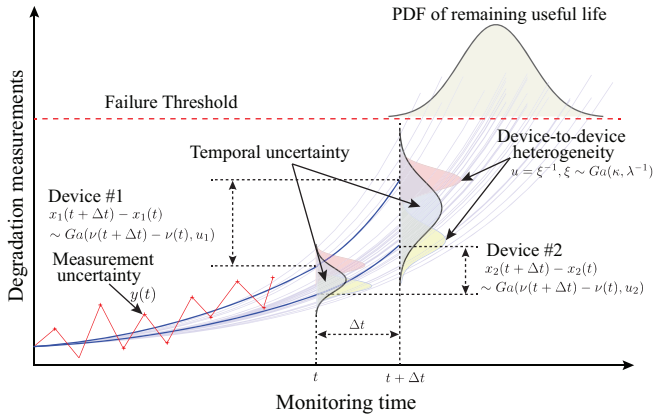

Fig. 2. Degradation modeling mechanism with three-source uncertainties for condition monitoring of power devices. Temporal uncertainty is facilitated by modeling the health state $x(t)$ with a Gamma process. Measurement uncertainty is facilitated with the state-space framework considering the noisy degradation measurements $y(t)$. Device-to-device heterogeneity is facilitated by a device-specific random effect parameter u in the model.

$$x(t+\Delta t)-x(t)\sim Ga(\nu(t+\Delta t)-\nu(t),u),\Delta t\ge 0. \quad (2)$$

The measurement model for the noisy degradation measurements $y(t)$ is developed as

$$y(t)=x(t)+\varepsilon, \quad (3)$$

where ε denotes the measurement noise. It is considered as a normally distributed variable with mean 0 and variance σ^2. To cover the device-to-device heterogeneity in a batch of power devices, the scale parameter u is assumed to be a random variable to model the random effect. A transformation is performed as $u=\xi^{-1}$, where $\xi\sim Ga(\kappa,\lambda^{-1})$ [29], for the mathematical tractability. As such, the random variable ξ possesses the mean κ/λ and the variance κ/λ^2.

Note that (2) is driven by a Gamma process. It is a stochastic process covering the temporal uncertainty with the monotonic increment and no equidistant requirement on the condition monitoring interval Δt. Such features theoretically justify aperiodic degradation measurements and monotonic health state changes. The noisy feature is facilitated by the state-space model consisting of (2) and (3). The device-to-device heterogeneity is characterized by a device-specific random effect parameter u. Fig. 2 presents the degradation modeling mechanism with three-source uncertainties for condition monitoring of power devices. As a result, in the proposed Gamma state-space framework, the monotonic health state can be iteratively estimated from the noisy and aperiodic degradation measurements. The PDF of the health state $x(t)$ can be developed as

$$\begin{aligned}f(x(t))&=\int_0^\infty f(x(t);\nu(t),\xi^{-1})\cdot f(\xi;\kappa,\lambda^{-1})d\xi\\&=\frac{\lambda^\kappa x(t)^{\nu(t)-1}}{B(\nu(t),\kappa)\cdot(x(t)+\lambda)^{\nu(t)+\kappa}},\end{aligned} \quad (4)$$

where $B(a,b)$ is the Beta function defined as $B(a,b)=\Gamma(a)\cdot\Gamma(b)/\Gamma(a+b)$, and the derivation details can be found in

This article has been accepted for publication in a future issue of this journal, but has not been fully edited. Content may change prior to final publication. Citation information: DOI 10.1109/TIM.2021.3054429, IEEE Transactions on Instrumentation and Measurement

Appendix A1. For any $t \geq 0$ and $\Delta t \geq 0$, define the health state increment $\Delta x(t) = x(t+\Delta t) - x(t)$. Similarly, from (4), it follows that the PDF of $\Delta x(t)$ can be developed as

$$f(\Delta x(t)) = \int_0^\infty f(\Delta x(t); \Delta\nu(t), \xi^{-1}) \cdot f(\xi; \kappa, \lambda^{-1}) d\xi = \frac{\lambda^\kappa \Delta x(t)^{\Delta\nu(t)-1}}{B(\Delta\nu(t), \kappa) \cdot (\Delta x(t) + \lambda)^{\Delta\nu(t)+\kappa}}, \quad (5)$$

where $\Delta\nu(t) = \nu(t+\Delta t) - \nu(t)$. Note that the health state $x(t)$ at CM time t and the corresponding future increment $\Delta x(t)$ are independent variables conditioned on the random effect term, i.e., the shape parameter u. Thus, the conditional PDF of $\Delta x(t)$ given the current health state $x(t)$ can be derived as

$$f(\Delta x(t) \mid x(t)) = \frac{f(\Delta x(t), x(t))}{f(x(t))} = \frac{(\Delta x(t))^{\Delta\nu(t)-1}(x(t)+\lambda)^{\nu(t)+\kappa}}{B(\nu(t)+\kappa, \Delta\nu(t))(x(t)+\Delta x(t)+\lambda)^{\nu(t)+\Delta\nu(t)+\kappa}}. \quad (6)$$

The derivation details are given in Appendix A2.

Corollary 1. *Assume a random variable as* $\zeta = \frac{\nu(t)+\kappa}{\Delta\nu(t)} \cdot \frac{\Delta x(t)}{x(t)+\lambda}$. *Conditioned on the current health state* $x(t)$, $\zeta \sim \mathcal{F}_{2\Delta\nu(t),2\nu(t)+2\kappa}$ [29].

The proof is provided in Appendix A3.

Let the failure time T_F be the time instant when the health state exceeds the predefined critical level x_F. Given that a power device works properly at CM time instant t, with Corollary 1, the conditional cumulative probability function (CDF) of T_F given the current degradation level $x(t)$ can be developed as

$$\begin{aligned} &P(T_F > t + \Delta t \mid T_F > t, x(t)) \\ &= P(\Delta x(t) < x_F - x(t) \mid x(t)) \\ &= \int_0^{x_F - x(t)} f(\Delta x(t) \mid x(t)) d\Delta x(t) \\ &= F\left(\frac{(\nu(t)+\kappa)(x_F - x(t))}{\Delta\nu(t)(x(t)+\lambda)}\right), \end{aligned} \quad (7)$$

where $F(\cdot)$ is the CDF of $\mathcal{F}_{2\Delta\nu(t_R),2\nu(t)+2\kappa}$. Thus, the PDF of the RUL t_R can be developed as

$$f_{T_R}(t_R \mid T_F > t, x(t)) = \frac{dF\left(\frac{(\nu(t)+\kappa)(x_F-x(t))}{\Delta\nu(t)(x(t)+\lambda)}\right)}{dt_R} = \left(\frac{(x_F - x(t))^{\Delta\nu(t_R)}(x(t)+\lambda)^{\nu(t)+\kappa}}{B(\nu(t)+\kappa, \Delta\nu(t_R))(x_F+\lambda)^{\nu(t)+\Delta\nu(t_R)+\kappa}\Delta\nu(t_R)} \cdot \frac{d\nu(t+t_R)}{dt_R}\right). \quad (8)$$

As a result, explicit health assessment characteristics and RUL prediction are obtained based on the framework of the Gamma state-space model. Subsequently, a parameter estimation method is proposed for device characterization.

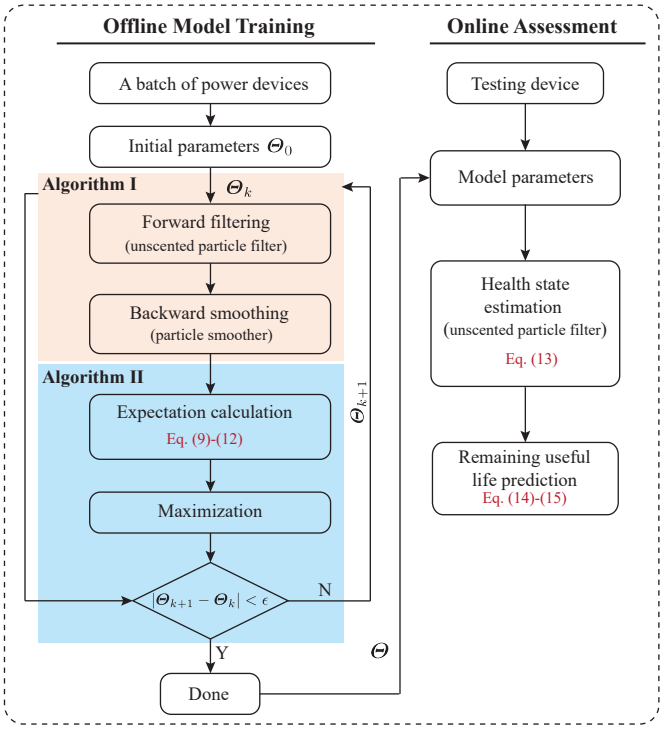

Fig. 3. Flowchart of the proposed method of model parameter estimation.

III. Model Parameter Estimation

Fig. 3 presents a flowchart to show the procedures of the proposed Gamma state-space model with a condition monitoring dataset of power devices. It typically consists of two parts:

1) *Offline Model Training*: The offline model training aims to quantify informative knowledge shared in a batch of power devices. A model parameter estimation method is developed to estimate the unknown parameter set $\boldsymbol{\Theta} = \{\nu(t), \kappa, \lambda, \sigma^2\}$ in (2) and (3) based on the health states estimated from the noisy and aperiodic degradation measurements. As a result, the degradation behavior of the device population is characterized by $\boldsymbol{\Theta}$.
2) *Online Assessment*: The online assessment refers to the model updates for a specific power device in service for the individual health state estimation and RUL prediction. With $\boldsymbol{\Theta}$, the Gamma state-space model is able to adaptively predict the future health state for RUL prediction with the latest measurements.

The method in the offline model training is twofold. Firstly, to facilitate the likelihood function calculation, an unscented particle filter-smoother method is derived to estimate the health states from the noisy and aperiodic degradation measurements. Secondly, considering the health states are hidden in the noisy degradation measurements, the conventional method of maximum likelihood cannot be directly applied to estimate the model parameters. Instead, a stochastic expectation-maximization (SEM) algorithm is developed to calculate the model parameter by iteratively performing the expectation of the log-likelihood function step (E-step) and maximization step (M-step). These two parts are detailed subsequently.

This article has been accepted for publication in a future issue of this journal, but has not been fully edited. Content may change prior to final publication. Citation information: DOI 10.1109/TIM.2021.3054429, IEEE Transactions on Instrumentation and Measurement

A. Unscented Particle Filter-Smoother Method

Particle filter (PF) is a sequential Monte Carlo method to estimate state for non-Gaussian and nonlinear models. One of the critical factors determining the accuracy is the quality of the proposal function [32]. For mathematical and computational convenience, the proposal distribution is typically determined as the transition prior, and thus the latest measurements are usually neglected. This strategy will fail when the new measurements appear in the tail of the prior distribution, or the likelihood is rather peak. Such cases commonly occur in the condition monitoring of power devices. One solution is applying the unscented Kalman Filter (UKF) [33] in the design of the proposal distribution, where the approximation errors can be scaled and the posterior covariance can be calculated accurately up to second order. By integrating the UKF into the PF framework, an unscented particle filter (UPF) [33] can be applied to isolate the health state from the noisy measurements with the proposed Gamma state-space model. Note that UPF is a forward filtering technique considering only the measurements up to current monitoring time when approximating the posterior distribution. In order to exploit the whole CM sequence, a particle smoothing technique [34] for backward smoothing is applied subsequently to improve the state estimation accuracy further. In this way, an unscented particle filter-smoother technique is proposed.

With the degradation measurements of m power devices, for ith device, suppose that it is inspected at CM time instants $0 = t_{i,0} < t_{i,1} < \cdots < t_{i,j} < \cdots < t_{i,n_i} < \infty$, $i = 1, ..., m$, $j = 1, ..., n_i$. At CM time instant $t_{i,j}$, the health state is denoted as $x_{i,j} = x(t_{i,j})$, $x(t_{i,0}) = 0$, and the health state increment during $(t_{i,j-1}, t_{i,j})$ is defined as $\Delta x_{i,j} = x(t_{i,j}) - x(t_{i,j-1})$. Note that $\nu_{i,j} = \nu(t_{i,j})$, $\nu(t_{i,0}) = 0$, and $\Delta\nu_{i,j} = \nu(t_{i,j}) - \nu(t_{i,j-1})$. The model parameters are united as a parameter set $\boldsymbol{\Theta} = \{\nu(t), \kappa, \lambda, \sigma^2\}$. The unscented particle filter-smoother method is presented as Algorithm I.

Algorithm I: Unscented Particle Filter-Smoother

Input: $\boldsymbol{\Theta} = \{\nu(t), \kappa, \lambda, \sigma^2\}$, $y_{i,1:n_i} = \{y_{i,j}, j = 1, \cdots, n_i\}$, $i = 1, \cdots, m$.

Output: $s_{i,1:n_i}^{1:N} = \{s_{i,j}^{1:N}, j = 1, \cdots, n_i\}$, $i = 1, \cdots, m$.

• *Part I-Unscented Particle Filter for forward filtering*

1. Initialization:

For i^{th} device, generate N random particles that are denoted as $x_{i,0}^d$, $d = 1, \cdots, N$ from the prior $p(x_{i,0})$. Also, set the augmented mean $\bar{x}_{i,0}^{(d)a} = E[x_{i,0}^{(d)a}] = [\bar{x}_{i,0}^{(d)} \quad 0 \quad 0]^T$ and the augmented covariance matrix $P^{(d)a} = E[(x_{i,0}^{(d)a} - \bar{x}_{i,0}^{(d)a})(x_{i,0}^{(d)a} - \bar{x}_{i,0}^{(d)a})^T] = diag(P_0^{(d)} \quad 0 \quad \sigma^2)$.

2. For $j = 1, \cdots, n_i$, update the particles with the following steps.

(a) Calculate the sigma points $\chi_{j-1}^{(d)a}$ and the corresponding weights w using the scaled unscented transformation as

$$\chi_{j-1}^{(d)a} = [\bar{x}_{i,j-1}^{(d)a} \quad \bar{x}_{i,j-1}^{(d)a} \pm \sqrt{(n_a + \lambda)P_{j-1}^{(d)a}}],$$

$$w_0^{(m)} = \frac{\lambda}{n_x + \lambda},$$

$$w_0^{(c)} = \frac{\lambda}{n_x + \lambda} + (1 - \alpha^2 + \beta),$$

$$w_k^{(m)} = w_k^{(c)} = \frac{1}{2(n_x + \lambda)}, k = 1, \cdots, 2n_x,$$

where $x_{i,0} \in \mathbf{R}^{n_x}$ and $n_a = n_x + 1$. In this case, $n_x = 1$ and thus $n_a = 2$.

(b) Time update to propagate particles

$$\chi_{j|j-1}^{(d)x} = \mathbf{f}(\chi_{j-1}^{(d)x}), \bar{x}_{j|j-1}^{(d)} = \sum_{k=0}^{2n_a} w_k^{(m)} \chi_{k,j|j-1}^{(d)x},$$

$$P_{j|j-1}^{(d)} = \sum_{k=0}^{2n_a} w_k^{(c)} [\chi_{k,j|j-1}^{(d)x} - \bar{x}_{j|j-1}^{(d)}][\chi_{k,j|j-1}^{(d)x} - \bar{x}_{j|j-1}^{(d)}]^T,$$

$$y_{j|j-1}^{(d)} = \mathbf{h}(\chi_{j|j-1}^{(d)x}, \chi_{j-1}^{(d)n}), \bar{y}_{j|j-1}^{(d)} = \sum_{k=0}^{2n_a} w_k^{(m)} y_{k,j|j-1}^{(d)},$$

where $\chi^a = [(\chi^x)^T 0^T (\chi^n)^T]^T$, $\mathbf{f}(\cdot)$ is the state transition function (2) and $\mathbf{h}(\cdot)$ is the measurement function (3).

(c) Measurement update to incorporate the new degradation measurements

$$P_{\tilde{y}_j \tilde{y}_j} = \sum_{k=0}^{2n_a} w_k^{(c)} [y_{k,j|j-1}^{(d)} - \bar{y}_{j|j-1}^{(d)}][y_{k,j|j-1}^{(d)} - \bar{y}_{j|j-1}^{(d)}]^T,$$

$$P_{x_j y_j} = \sum_{k=0}^{2n_a} w_k^{(c)} [\chi_{k,j|j-1}^{(d)} - \bar{x}_{j|j-1}^{(d)}][y_{k,j|j-1}^{(d)} - \bar{y}_{j|j-1}^{(d)}]^T,$$

$$K_j = P_{x_j y_j} P_{\tilde{y}_j \tilde{y}_j}^{-1}, \bar{x}_j^{(d)} = \bar{x}_{j|j-1}^{(i)} + K_j(y_j - \bar{y}_{j|j-1}^{(d)}),$$

$$\hat{P}_j^{(d)} = P_{j|j-1}^{(d)} - K_j P_{\tilde{y}_j \tilde{y}_j} K_j^T.$$

(d) Sample the particles from $\hat{x}_j^{(d)} \sim q(x_j^{(d)} \mid x_{0:j-1}^{(d)}, y_{1:j}) = N(\bar{x}_j^{(d)}, \hat{P}_j^{(d)})$.

(e) Calculate the importance weights as

$$w_j^{(d)} \propto \frac{p(y_j \mid \hat{x}_j^{(d)}) p(\hat{x}_j^{(d)} \mid x_{j-1}^{(d)})}{q(x_j^{(d)} \mid x_{0:j-1}^{(d)}, y_{1:j})},$$

and then normalize the weights.

(f) Obtain $x_j^{1:N}$ by improving particle quality with resampling technique.

• *Part II-Particle Smoother for backward smoothing*

1. At $j = n_i$, obtain the smoother $s_{n_i}^{1:N}$ using the resample technique with w_{n_i}.

2. For $j = n_i - 1, \cdots, 1$, obtain the smoothers as

(a) For each $d = 1, \cdots, N$, calculate the smoother weights using $w_{j|j+1}^{(d)} = w_j^{(d)} f(s_{j+1} \mid x_j^{(d)})$.

(b) Normalize the $w_{j|j+1}^{(d)}$.

(c) Obtain $s_j^{1:N}$ using resample technique in terms of the normalized weights $w_{j|j+1}^{(d)}$.

• *Loop Part I and Part II respectively in terms of* $i = 1, \cdots, m$.

Fig. 4 presents the mechanism of the forward filtering and backward smoothing. For each device in the population, it can be seen in Part I that unscented particle filter is firstly applied to estimate the hidden health state from the noisy and

This article has been accepted for publication in a future issue of this journal, but has not been fully edited. Content may change prior to final publication. Citation information: DOI 10.1109/TIM.2021.3054429, IEEE Transactions on Instrumentation and Measurement

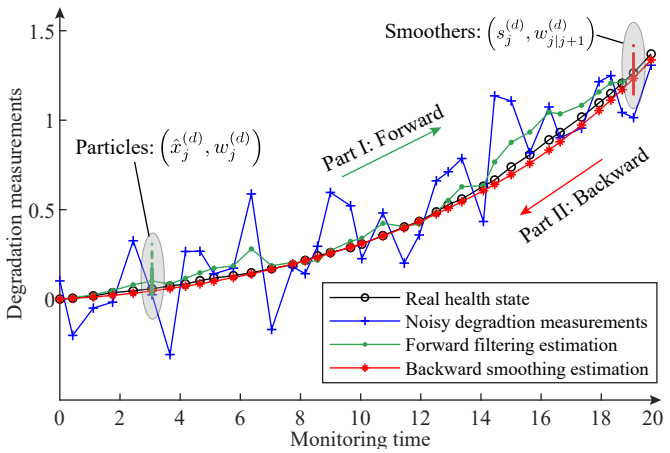

Fig. 4. Forward filtering and backward smoothing in Algorithm I. The estimation accuracy is improved by the backward smoothing compared with that of the forward filtering.

aperiodic degradation measurements, where the health states are estimated iteratively in a forward way. Subsequently, to improve the estimation accuracy, Part II particle smoother is performed based on the estimated health state in a backward way to improve the estimation accuracy. As a result, Algorithm I can estimate the hidden health states accurately for the subsequent model parameter estimation. More technical details of Part I unscented particle filter can be found in [33], and more technical details of Part II particle smoother can be found in [34].

B. Stochastic Expectation-Maximization Method

Note that the health state is not directly observable and therefore analytically developing the likelihood function is infeasible. The SEM algorithm [28], [35] is able to tackle the parameter estimation in the case of the unobservable health states. It deals with iterative operations of two steps, i.e., the calculation of the expectation of the log-likelihood function, and the maximization of the expectation, respectively. Considering the independent increment property, the likelihood function can be developed based on (5) as

$$\begin{aligned} L(\boldsymbol{\Theta}) =& \prod_{i=1}^{m} f(\Delta x_{i,1}, \cdots, \Delta x_{i,n_i}) \\ =& \prod_{i=1}^{m} \int_0^{\infty} \prod_{j=1}^{n_i} f(\Delta x_{i,j}; \Delta\nu_{i,j}, \xi^{-1}) \cdot f(\xi; \kappa, \lambda^{-1}) d\xi \\ =& \prod_{i=1}^{m} \left\{ \frac{\lambda^{\kappa}\Gamma(\kappa+\nu_{i,n_i})}{\Gamma(\kappa)\prod_{j=1}^{n_i}\Gamma(\Delta\nu_{i,j})} \cdot \frac{\prod_{j=1}^{n_i} \Delta x_{i,j}^{\Delta\nu_{i,j}-1}}{(\lambda+x_{i,n_i})^{\kappa+\nu_{i,n_i}}} \right\}. \end{aligned} \tag{9}$$

The expectation of the log-likelihood function can be decomposed into two parts as

$$E\left[\log(L(\boldsymbol{\Theta}))\right] = E\left[\log(\prod_{i=1}^{m} f(y_{i,1:n_i}, x_{i,1:n_i} \mid \boldsymbol{\Theta}))\right] \tag{10}$$

$$\begin{aligned} &= E\left[\log(\prod_{i=1}^{m} (f(y_{i,1:n_i} \mid x_{i,1:n_i}, \boldsymbol{\Theta}) \cdot f(x_{i,1:n_i} \mid \boldsymbol{\Theta})))\right] \\ &= E\left[\log(\prod_{i=1}^{m} f(x_{i,1:n_i} \mid \boldsymbol{\Theta}_1))\right] \rightarrow \text{First part} \\ &+ E\left[\log(\prod_{i=1}^{m} f(y_{i,1:n_i} \mid x_{i,1:n_i}, \boldsymbol{\Theta}_2))\right], \rightarrow \text{Second part} \end{aligned}$$

where $\boldsymbol{\Theta} = \{\boldsymbol{\Theta}_1, \boldsymbol{\Theta}_2\}$, $\boldsymbol{\Theta}_1 = \{\nu(t), \kappa, \lambda\}$, and $\boldsymbol{\Theta}_2 = \{\sigma^2\}$. Note that the first part is only involved with the health state. It can be further developed as

$$\begin{aligned} & E\left[\log(\prod_{i=1}^{m} f(x_{i,1:n_i} \mid \boldsymbol{\Theta}_1))\right] \\ =& \sum_{i=1}^{m} E\left[\log(f(x_{i,1:n_i} \mid \boldsymbol{\Theta}_1))\right] \\ =& \sum_{i=1}^{m} \begin{pmatrix} \kappa\log\lambda + \log\Gamma(\kappa+\nu_{i,n_i}) - \log\Gamma(\kappa) \\ -\sum_{j=1}^{n_i}\log\Gamma(\Delta\nu_{i,j}) + \sum_{j=1}^{n_i}(\Delta\nu_{i,j}-1)E\left[\log\Delta x_{i,j}\right] \\ -(\kappa+\nu_{i,n_i})E\left[\log(\lambda+x_{i,n_i})\right] \end{pmatrix}, \end{aligned} \tag{11}$$

The derivation details are given in Appendix A4.

The second part is formulated as

$$\begin{aligned} & E\left[\log(\prod_{i=1}^{m} f(y_{i,1:n_i} \mid x_{i,1:n_i}, \boldsymbol{\Theta}_2))\right] \\ =& \sum_{i=1}^{m}\sum_{j=1}^{n_i} \begin{pmatrix} \frac{1}{2}\log(2\pi\sigma^2) \\ -\frac{1}{2\sigma^2}\left(y_{i,j}^2 - 2y_{i,j}E\left[x_{i,j}\right] + E\left[x_{i,j}^2\right]\right) \end{pmatrix}. \end{aligned} \tag{12}$$

The derivation details are given in Appendix A5. For the expectation terms in (11) and (12), they can be obtained with Algorithm I as

$$\begin{cases} E\left[\log\Delta x_{i,j}\right] = \frac{1}{N}\sum_{d=1}^{N}\log(s_{i,j}^{(d)} - s_{i,j-1}^{(d)}), \\ E\left[\log(\lambda+x_{i,n_i})\right] = \frac{1}{N}\sum_{d=1}^{N}\log(\lambda+s_{i,n_i}^{(d)}), \\ E\left[x_{i,j}\right] = \frac{1}{N}\sum_{d=1}^{N} s_{i,j}^{(d)}, \\ E\left[x_{i,j}^2\right] = \frac{1}{N}\sum_{d=1}^{N}(s_{i,j}^{(d)})^2. \end{cases} \tag{13}$$

In this way, the expectation of the log-likelihood function can be calculated. Subsequently, the maximization procedure is performed on (10) to start the iterative loop. Several standard procedures, including GlobalSearch, fminsearch [36], and Bayesian MCMC [13], can be applied to optimize the likelihood function. The whole SEM method is elaborated as Algorithm II.

Algorithm II: Stochastic Expectation-Maximization Method

This article has been accepted for publication in a future issue of this journal, but has not been fully edited. Content may change prior to final publication. Citation information: DOI 10.1109/TIM.2021.3054429, IEEE Transactions on Instrumentation and Measurement

Input: $s_{i,1:n_i}^{1:N} = \{s_{i,j}^{1:N}, j = 1, \cdots, n_i\}$, $y_{i,1:n_i} = \{y_{i,j}, j = 1, \cdots, n_i\}$, $i = 1, \cdots, m$.
Output: $\boldsymbol{\Theta} = \{\nu(t), \kappa, \lambda, \sigma^2\}$.

1. Determine the initials $\boldsymbol{\Theta}_0$.
2. E-step: For $k \geq 1$, calculate the expectation of the log-likelood function using (10) with $\boldsymbol{\Theta}_k$.
3. M-Step: perform the optimization procedure to find $\boldsymbol{\Theta}_{k+1}$ such that

$$\boldsymbol{\Theta}_{k+1} = \underset{\boldsymbol{\Theta}}{\operatorname{argmax}} \left\{ E\left[\log(L(\boldsymbol{\Theta}))\right] \right\}.$$

4. Loop step 2 and step 3 respectively until $\| \boldsymbol{\Theta}_{k+1} - \boldsymbol{\Theta}_k \| \leq \epsilon$, where ϵ is a small enough threshold value.
5. Return $\boldsymbol{\Theta}_{k+1}$.

C. Remaining Useful Life Prediction

With the estimated model parameters, the proposed framework can provide health assessment for a specific power device in service. For ith power device, given the estimated parameters $\boldsymbol{\Theta}$ and the CM sequence up to time $t_{i,j}$, the survival function at CM time instant $t_{i,j}$ can be derived as

$$\begin{aligned} & P(T_F > t \mid T_F > t_{i,j}, y_{i,1:j}) \\ &= \int_0^{x_F} \begin{pmatrix} P(T_F > t_{i,j} + \Delta t \mid T_F > t_{i,j}, x_{i,j}) \\ \cdot f(x_{i,j} \mid T_F > t_{i,j}, y_{i,j}) dx_{i,j} \end{pmatrix} \\ &\approx \frac{1}{N} \sum_{d=1}^{N} P(T_F > t_{i,j} + \Delta t \mid T_F > t_{i,j}, x_{i,j}^{(d)}) \\ &= \frac{1}{N} \sum_{d=1}^{N} F\left(\frac{(\nu(t_{i,j}) + \kappa)(x_F - x_{i,j}^{(d)})}{(\nu(t) - \nu(t_{i,j}))(x_{i,j}^{(d)} + \lambda)} \right). \end{aligned} \tag{14}$$

Accordingly, the RUL t_R of this specific device can be formulated as

$$\begin{aligned} & f_{T_R}(t_R \mid T_F > t_{i,j}, y_{i,j}) \\ &= \int_0^{x_F} f_{T_R}(t_R \mid T_F > t_{i,j}, x_{i,j}) f(x_{i,j} \mid T_F > t_{i,j}, y_{i,j}) dx_{i,j} \\ &\approx \frac{1}{N} \sum_{d=1}^{N} f_{T_R}(t_R \mid T_F > t_{i,j}, x_{i,j}^{(d)}) \\ &= \frac{1}{N} \sum_{d=1}^{N} \frac{(x_F - x_{i,j}^{(d)})^{\Delta\nu(t_R)} (x_{i,j}^{(d)} + \lambda)^{\nu(t_{i,j}) + \kappa}}{\begin{pmatrix} B(\nu(t_{i,j}) + \kappa, \Delta\nu(t_R)) \\ \cdot (x_F + \lambda)^{\nu(t_{i,j}) + \Delta\nu(t_R) + \kappa} \Delta\nu(t_R) \end{pmatrix}} \\ &\cdot \frac{d\nu(t_{i,j} + t_R)}{dt_R}. \end{aligned} \tag{15}$$

D. Numerical Verification

In this Section, a numerical study is designed to verify the accuracy and robustness of the proposed Gamma state-space method. The degradation measurements of a total of 30 units are simulated with (2) and (3) by using the Gamma-increment sampling technique [30]. For the simulation settings, the time-varying shape parameter is $\nu(t) = \exp(a + b \cdot t)$, where $a = 4.48$ and $b = 0.12$. The parameters for covering the heterogeneity are determined as $\kappa = 8.45$, and $\lambda = 0.0193$. To illustrate the robustness of the method, three different noisy levels, including the low-level, medium-level, and high-level, are considered with the variances of measurement noise σ^2 being 0.001, 0.02, and 0.05, respectively. It is worth mentioning that these parameters are randomly selected for illustration purposes. The results of several simulations show similar performances. Note that the proposed method is capable of tackling the aperiodic CM, for each simulated degradation path, it is randomly resampled to generate aperiodic CM sequences. As a result, the simulated paths of degradation measurements for the high-level case are shown in Fig. 5. Since it is a numerical simulation, the degradation measurements and the monitoring time are dimensionless. Thus, there are no units in the figures of the numerical study.

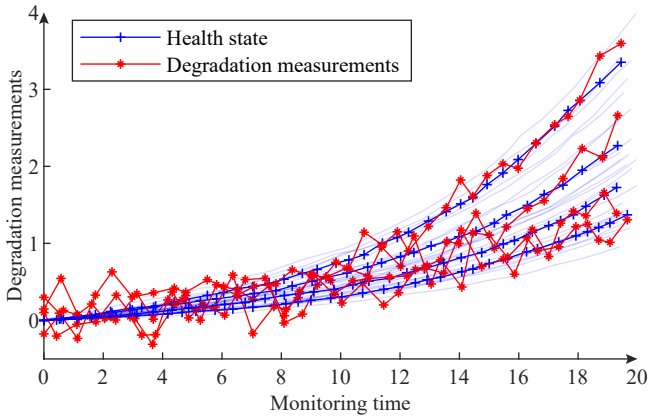

Fig. 5. Simulated paths of noisy and aperiodic degradation measurements of 30 units (high-level noise case). For illustrative clarity, four units are randomly selected and highlighted. For other units, the health state path is shown as a gray line.

Based on the simulated degradation measurements, the SEM algorithm is performed to obtain the model parameters. The initial parameter set $\boldsymbol{\Theta}_0$ are randomly determined to start the iterative loop in the SEM. To ensure the estimation accuracy of the unscented particle filter-smoother algorithm, the number of the particles is determined as 1000. The process of model parameter estimation of the high-level noise case is shown in Fig. 6. It can be seen that the process remains stable after 313 loops, and thus the SEM algorithm is considered to be converged with a convergence stop threshold $\epsilon = 0.0005$. The estimated model parameters with standard deviations are given in Table I for the three levels of noise. It is observed that the estimations of the unknown model parameters eventually converge to their true values. For different noisy levels, it is found that the estimation accuracy decreases with a higher noise level, as expected. Note that the converged model parameters κ, λ are not quite close to the predefined true values. The reason is that the estimated standard deviation of κ, λ are more significant than those of other parameters. As indicated by the simulations, such uncertainties can be reduced by increasing the number of training units. As a result, it is clearly shown that all the estimation errors are small, which demonstrates the method effectiveness and accuracy.

This article has been accepted for publication in a future issue of this journal, but has not been fully edited. Content may change prior to final publication. Citation information: DOI 10.1109/TIM.2021.3054429, IEEE Transactions on Instrumentation and Measurement

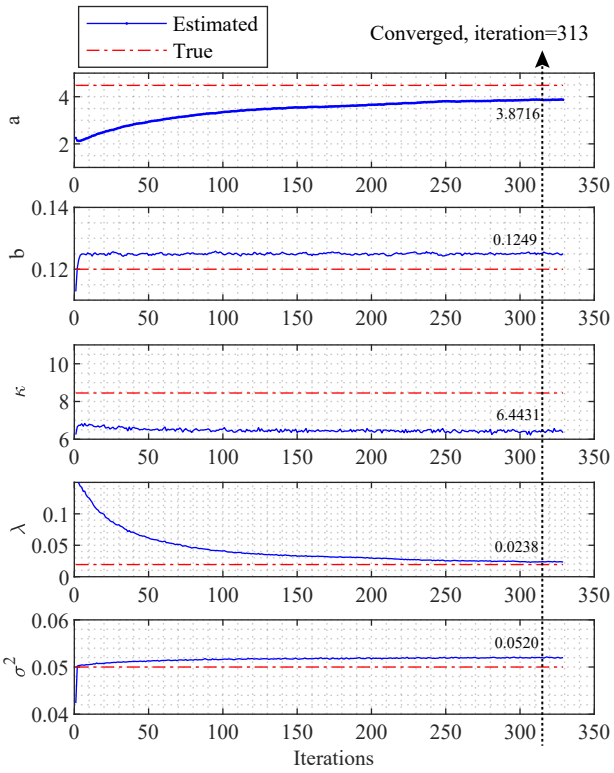

Fig. 6. Process of the model parameter estimation for a, b, σ^2, κ, λ (high-level noise case).

Table I: Performance of the model parameter estimation and the root mean square error (RMSE) of the health state estimation (N/A: not applicable)

Model parameters	True value	Estimated value (Standard deviation)		
		Low (σ^2=0.005)	Medium (σ^2=0.02)	High (σ^2=0.05)
a	4.48	4.5534 (0.0490)	4.3384 (0.0499)	3.8716 (0.0520)
b	0.12	0.1197 (0.0012)	0.1215 (0.0013)	0.1249 (0.0016)
κ	8.45	6.2243 (1.6808)	6.2935 (1.7587)	6.4431 (1.7496)
λ	0.0193	0.0128 (0.0037)	0.0154 (0.0047)	0.0238 (0.0071)
σ^2	N/A	0.0048 (2.16e-4)	0.0196 (8.57e-4)	0.0520 (0.0023)
RMSE	N/A	0.0215	0.0351	0.0498

Note that the procedure is performed several times with various random initials $\boldsymbol{\Theta}_0$ to avoid the possible local optimal results. All of the initials end with almost identical results, which shows the global convergence of the parameter estimation method.

1) Health State Estimation and Prediction: For illustration, with the estimated model parameters, unit #6 is randomly selected and the corresponding estimated health state in terms of three levels of noise is shown in Fig. 7. It can be seen that the estimated health state from the noisy degradation measurements agrees well with the corresponding real ones at different noise levels.

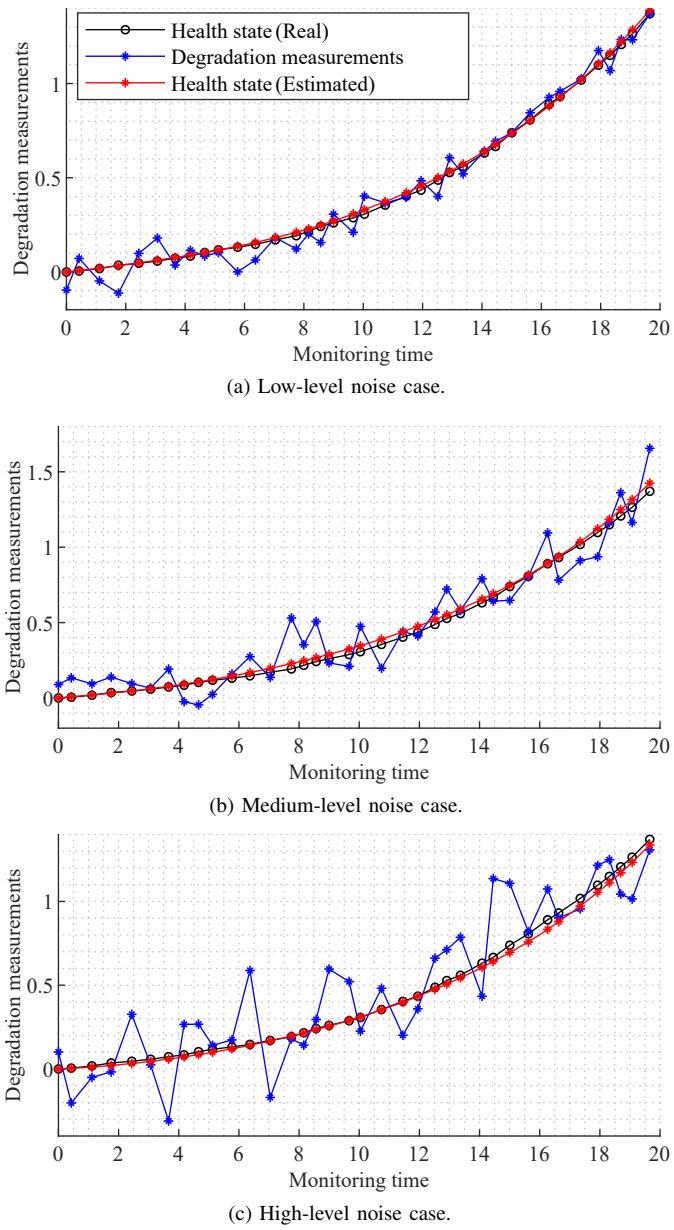

(a) Low-level noise case.

(b) Medium-level noise case.

(c) High-level noise case.

Fig. 7. Estimated health state from the noisy and aperiodic degradation measurements at different noisy levels for unit #6.

To quantitatively evaluate the health state estimation accuracy, the root mean square error (RMSE) of the health state of all the simulated units is defined as

$$\text{RMSE} = \sqrt{\frac{\sum_{i=1}^{m}\sum_{j=1}^{n_i}(\hat{x}_{i,j} - x_{i,j})^2}{\sum_{i=1}^{m} n_i}}, \tag{16}$$

where $\hat{x}_{i,j}$ is the estimated health state for unit i at CM time $t_{i,j}$. The results are presented in Table I. It can be seen that the RMSE tends to grow as the level of noise increases, as expected. For the high-level noise case, it is less than 3% (0.0498/2=2.49%) of the total degradation (its median equals to 2 approximately) in terms of the whole lifetime. The error is small, demonstrating the effectiveness of the parameter estimation method. As a result, the proposed

This article has been accepted for publication in a future issue of this journal, but has not been fully edited. Content may change prior to final publication. Citation information: DOI 10.1109/TIM.2021.3054429, IEEE Transactions on Instrumentation and Measurement

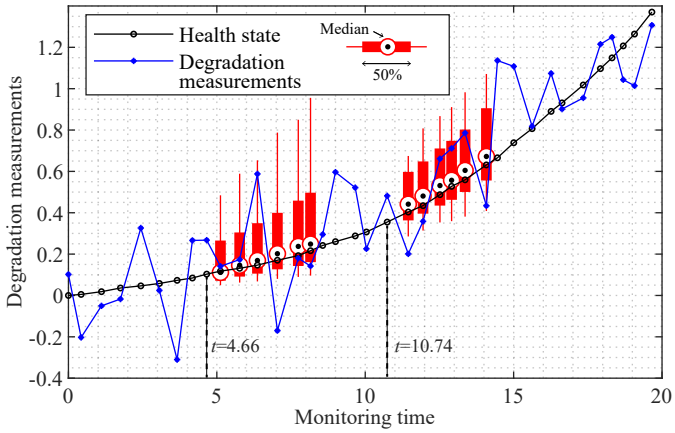

Fig. 8. Six steps ahead increment prediction of health state for unit #6 in the high-level noise case.

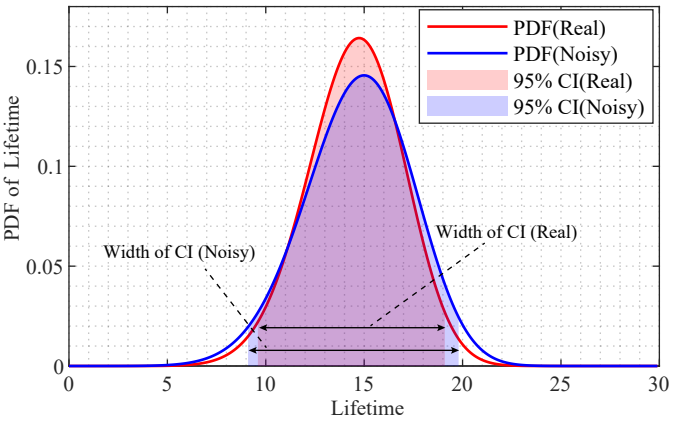

Fig. 9. Comparison of lifetime estimation by using the real health state (Real) and the estimated health state (Noisy) from the noisy degradation measurements.

method can isolate the monotonic health state increment from the degradation measurements.

For prediction performance, Fig. 8 shows the health state prediction with the unscented particle filter at CM time 4.66 and 10.74, respectively. The prediction is conducted for six monitoring time instants ahead of the current monitoring time. The boxplot indicates that the predicted medians of health states are almost identical to the real ones. The predicted 50% confidence interval (CI) covers the real health state well, which demonstrates the effectiveness of the health state prediction.

2) Lifetime Estimation and RUL Prediction: Fig. 9 presents the lifetime estimations by using the real health state and the estimated health state. It can be seen that the majority area of their 95% confidence intervals is overlapped. It suggests that a comparable lifetime estimation can be obtained using the degradation measurements with the proposed method. For practical applications, the original noisy CM signals can be safely applied to the lifetime estimation with the proposed method.

In addition to the lifetime estimation, the RUL prediction for unit in service can be performed as the CM time progresses according to (15). Here, the method of leave-one-out cross-validation [11] is applied to illustrate the performance of

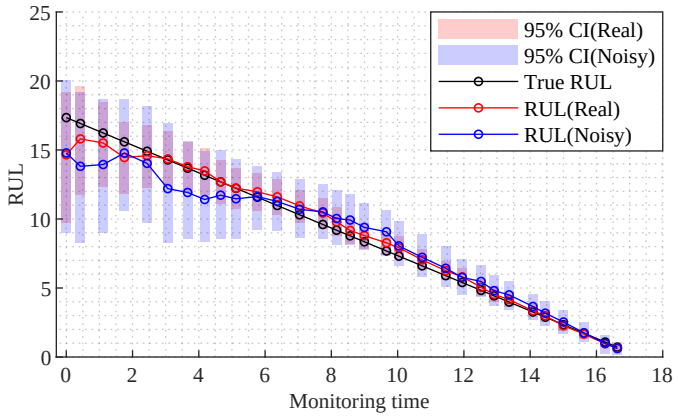

(a) Low-level noise case.

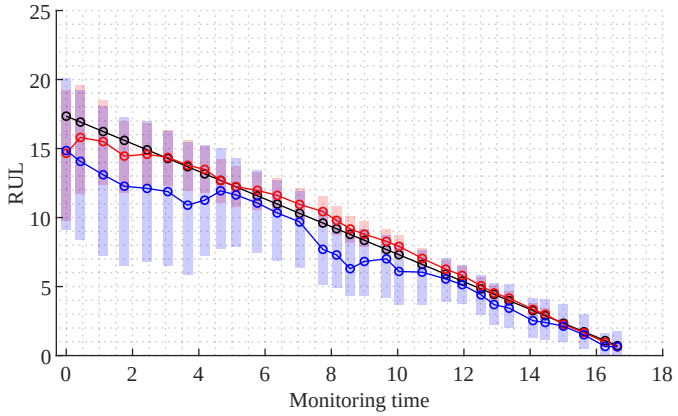

(b) Medium-level noise case.

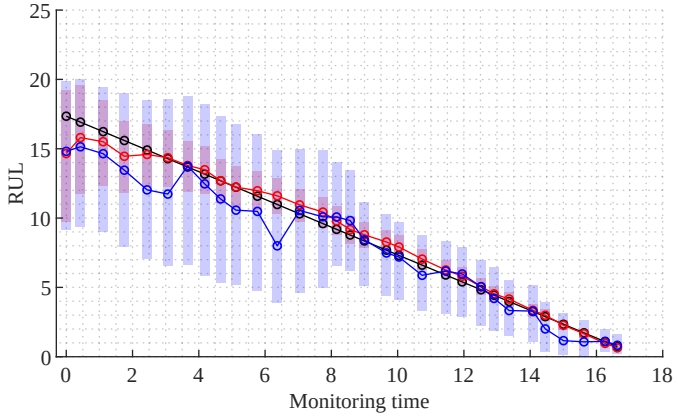

(c) High-level noise case.

Fig. 10. Comparison of 95% CI of the remaining useful life (RUL) predictions by using the real health state (Real) and the estimated health state (Noisy) from the noisy degradation measurements at three different noise levels.

RUL prediction. Thus, one unit is randomly selected from the population and the rest is considered as the training dataset for the model parameter estimation. For illustration, unit #6 is randomly selected as the test unit and the performance of RUL prediction in terms of three levels of noise is shown in Fig. 10, and the details are given in Table II. Note that the failure threshold x_F is selected as 1.0179. Consider the health state are exactly known in the numerical simulation,

Table II: Comparisons of 95% CI of RUL with the real health state and the noisy degradation measurements

Monitoring	True	Real health state data		Low-level noise		Medium-level noise		High-level noise	
Time	RUL	Estimation	95% CI	Estimation	95% CI	Estimation	95% CI	Estimation	95% CI
0	17.35	14.65	[9.73, 19.20]	14.79	[9.00, 20.08]	14.85	[9.12, 20.08]	14.81	[9.20,19.89]
3.06	14.29	14.36	[12.29, 16.34]	12.20	[8.27, 16.95]	11.88	[6.50, 16.25]	11.73	[6.58, 18.61]
5.77	11.58	11.97	[10.58, 13.33]	11.62	[9.23, 13.82]	11.05	[7.42, 13.42]	10.48	[4.77, 16.08]
8.57	8.78	9.17	[8.19, 10.14]	9.93	[8.12, 11.75]	6.29	[4.33, 9.25]	9.82	[6.17, 13.44]
11.45	5.90	6.26	[5.57, 6.94]	6.43	[5.11, 8.05]	5.55	[3.89, 7.01]	6.18	[3.10, 8.33]
14.08	3.27	3.35	[2.91, 3.79]	3.66	[2.68, 4.56]	2.53	[1.32, 4.15]	3.29	[1.07, 5.16]
16.63	0.72	0.64	[0.47, 0.82]	0.61	[0.17, 1.10]	0.64	[0.07, 1.76]	0.82	[0.22, 1.62]

its time exceeding the failure threshold x_F can be identified as the failure time for determining the true RUL during the prediction. It can be seen that the RUL estimation based on the degradation model using the health state data agrees very well with the true RUL, and the corresponding 95% CI precisely covers the true RUL with a very narrow width. For example, at CM time instant 14.08, the predicted RUL based on the degradation model with real data is 3.35 with 95% CI [2.91, 3.79]. Considering the true RUL 3.27, it suggests that the the degradation model can accurately characterize the degradation behavior of units.

On the other hand, it can be seen that the RUL predictions estimated by the model characterized at all three different noise levels are close to the one characterized by the real health state, especially when the unit approaches its failure time. Also, the true RUL is within the estimated 95% percentile interval in most cases. For example, compared with the RUL estimation 0.64 at CM time instant 16.63 by using the model trained with the health state data, the RUL estimations (95% CI) for the low-level, medium-level, and high-level noises are 0.61 ([0.17, 1.10]), 0.64 ([0.07, 1.76]), and 0.82 ([0.22, 1.62]), respectively. It demonstrates that the device degradation behavior is accurately inferred from the noisy and aperiodic degradation measurements.

Note that the width of the estimated 95% CI increases with the increase of the noise level. It is more obvious when comparing Fig. 10(a) and Fig. 10(c). As expected, with higher noisy degradation measurements, the uncertainty level in the estimation of real health state increases and leads to a wider 95% CI in the RUL prediction. From a whole life cycle perspective, the 95% CI estimated by all of the three noise cases almost covers that estimated by the health state data. It demonstrates the robustness of the proposed method.

As the CM time progresses, the agreement performance of 95% CI by using the health state data and the estimated one is gradually decreasing. The reason is that when the unit approaches its end-of-life time, the sensitivity of the RUL prediction in terms of the estimated degradation level error increases considerably. Although the agreement performance decreases, the prediction results by using the noisy degradation measurements are still close to the real one. It indicates that the RUL prediction results provided by the proposed method can be safely applied to practical applications.

In addition to unit #6, using the metric in (16), the total RMSE in terms of the RUL prediction is calculated by performing the leave-one-out cross-validation method on each unit in the population. The results of the cases, including the health state data, low-level degradation measurements, medium-level degradation measurements, and high-level degradation measurements, are 0.96, 1.51, 1.77, and 1.92, respectively. It indicates that the RUL predictions are accurate for all three noisy cases, considering the whole life cycle is 17.35.

The numerical study indicates that the degradation behavior can be well characterized by the proposed Gamma state-space model. The reliability characteristics can be accurately estimated from the noisy and aperiodic degradation measurements.

IV. Health Assessment of SiC MOSFETs

As a promising device, SiC MOSFETs possess superior performances in high-voltage and high-power-density applications compared with conventional silicon-based ones. To illustrate the industrial effectiveness and potentials, the proposed framework is implemented on the condition monitoring of SiC MOSFETs to provide its health state estimation and RUL prediction in the presence of the noisy and aperiodic degradation measurements.

A. Accelerated Testing Experiment and Data Preparation

Power cycling is a practical approach to accelerate the device aging process for the reliability assessment in a reasonable period. The degradation dataset is essential to the failure precursor identification and failure mechanism analysis. For SiC MOSFETs, it indicates that the increment of drain-to-source on-state resistance $\Delta R_{\text{DS(on)}}$ is a degradation measurement. To obtain the SiC MOSFETs dataset, an accelerated testing experiment setup is designed as in Fig. 11.

The generation-II SiC MOSFETs (1.2 kV/10 A) are utilized in the experiment. For each iterative power cycling period, the device under test (DUT) without a heatsink, is actively heated up to the upper-junction-temperature limit 200°C by injecting half of the rated current (4.5A). Subsequently, the fan near the device is triggered to cool down to the lower-junction-temperature limit of 30°C. Each power cycling takes around three minutes consisting of one minute for heating and two minutes for cooling. Note that the temperature is directly obtained by the thermocouples attached to the metal tab of the device. The method of obtaining the junction temperature from the case temperature measured by the thermocouples can be found in [37]. After every 250 cycles, the device is removed and characterized by a curve tracer (Keysight B1506A) to record the $R_{\text{DS(on)}}$ at ambient temperature.

This article has been accepted for publication in a future issue of this journal, but has not been fully edited. Content may change prior to final publication. Citation information: DOI 10.1109/TIM.2021.3054429, IEEE Transactions on Instrumentation and Measurement

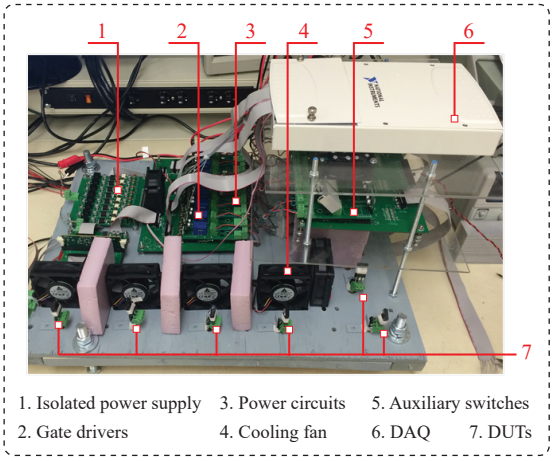

Fig. 11. Setup for the accelerated testing experiment of SiC MOSFETs [37].

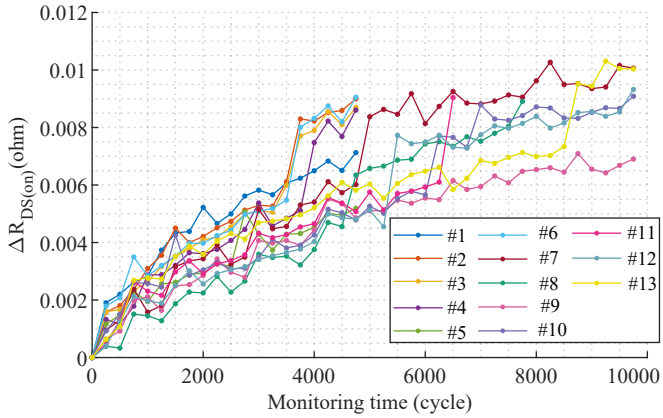

Fig. 12. $\Delta R_{\mathrm{DS(on)}}$ with the aging time for a total of 13 devices in the accelerated testing experiment. The $\Delta R_{\mathrm{DS(on)}}$ is considered as the degradation measurement in the framework.

The experiment has been conducted twice to obtain a sufficient sample size, where each experiment includes seven devices. The $R_{\mathrm{DS(on)}}$ is measured after each 250 power testing cycles until the end of the experiment, i.e., 5000 cycles for the first experiment and 10 000 cycles for the second one. Note that one of the devices in the first experiment, which shows exceptional degradation pattern due to the different failure mechanisms, is excluded from the device population. As a result, the degradation dataset with a total of 13 devices is applied to the subsequent analysis. More details of the accelerated testing experiment can be found in [4], [37], [38], and the degradation measurements of the increment of $\Delta R_{\mathrm{DS(on)}}$ are illustrated in Fig. 12.

Note that the initially collected dataset is a periodic case, i.e. the time between two consecutive data points is 250 cycles. To highlight the capability of the proposed method in dealing with the aperiodic CM scheme, for each periodic CM time series, some CM data points are randomly deleted. In this way, the time between some consecutive data points is multiples of 250 cycles (e.g., 500, 750, etc.), resulting in an aperiodic CM dataset. The deleted data points will not be used in the subsequent method verification. As a result, the degradation measurements of $\Delta R_{\mathrm{DS(on)}}$ for SiC MOSFETs are noisy and aperiodic. It is consistent with the model assumptions.

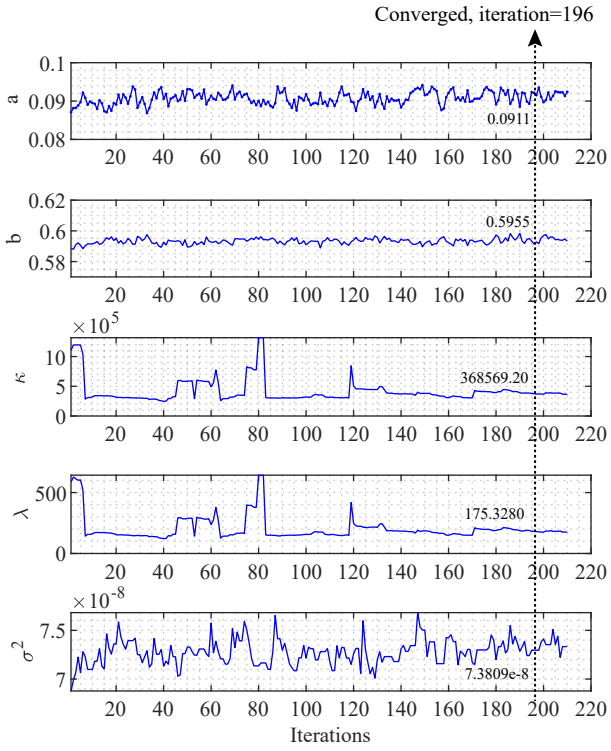

Fig. 13. Process of the model parameter estimation with the proposed stochastic expectation-maximization method.

B. Health State Estimation and RUL Prediction

Based on the data analysis of the pattern of $\Delta R_{\mathrm{DS(on)}}$ in Fig. 12, the time-varying shape parameter in (1) is determined as $\nu(t) = at^b$. Similar to the numerical example in Section III-D, the leave-one-out cross-validation is applied here. The model parameter set $\boldsymbol{\Theta}$ can be estimated according to Algorithms I and II. Fig. 13 presents the estimation process of the model parameter. According to the convergence criteria, the SEM algorithm runs to stable and is converged after 196 loops. The model parameters are determined as $a = 0.0911$, $b = 0.5955$, $\kappa = 368\,569.20$, $\lambda = 175.3280$, $\sigma^2 = 7.3809 \times 10^{-8}$.

As an online health assessment application of a specific SiC MOSFET in service, devices #8 and #9 are randomly selected for verification. Fig. 14 presents the estimated health states from noisy and aperiodic degradation measurements. It can be seen that the estimated health state is of better monotonicity compared with the noisy degradation measurements. It is better for indicating the health status of SiC MOSFETs and can better support the RUL prediction. Note that there is an abrupt change at monitoring time 4500 cycles to 4750 cycles for device #8. In this severe case, the proposed health state estimation method is still able to capture this rapid device behavior change. It is worth mentioning that whether the estimated health state is close to the degradation measurement does not matter. The key is that the abrupt changes of device behavior, which are partially related to the degradation measurements, can be indicated in the health state estimation as well.

This article has been accepted for publication in a future issue of this journal, but has not been fully edited. Content may change prior to final publication. Citation information: DOI 10.1109/TIM.2021.3054429, IEEE Transactions on Instrumentation and Measurement

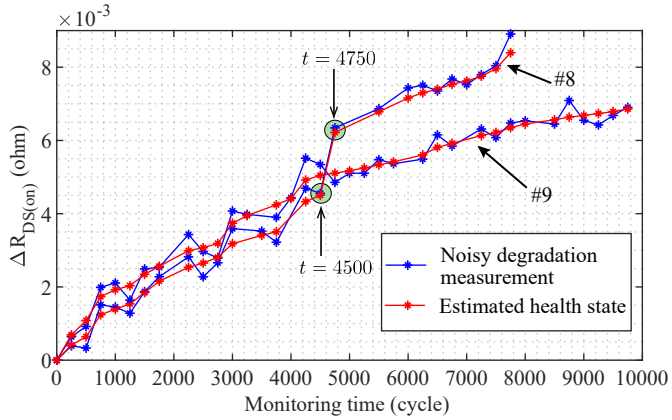

Fig. 14. Health state estimation from noisy and aperiodic $\Delta R_{\text{DS(on)}}$ for devices #8 and #9.

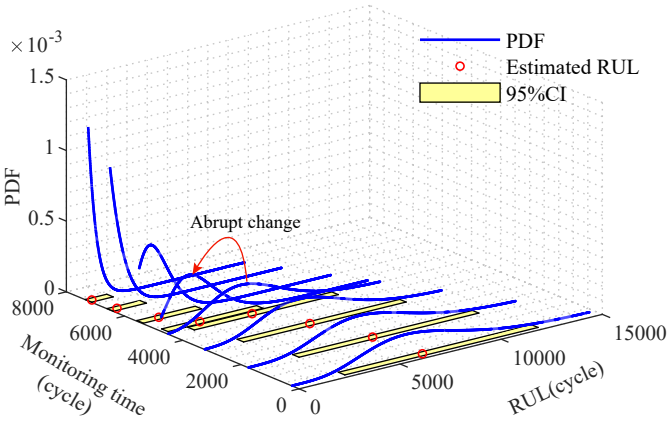

Fig. 15. RUL prediction by using the estimated health state at various CM time instants for device #8.

The failure threshold x_F is empirically determined as 0.0075 (ohm) for the RUL prediction. Fig. 15 presents the RUL estimation of device #8 at different CM time instants. It can be seen that the PDF of RUL gets narrower and the estimated RUL decreases with the CM time progresses. The decrease of the width of 95% CI indicates the lower uncertainty level as the device approaches its failure state. Note that there is an abrupt change of the PDF of RUL at CM time instants of 4500 cycles and 4750 cycles. It is due to the sudden increment of $\Delta R_{\text{DS(on)}}$, as shown in Fig. 14.

Table III presents the details of the RUL predictions. For example, given the current health state, the RUL is predicted as 180 cycles with 95% CI as $[160, 1077]$ cycles at monitoring time 7250 cycles. Due to the real health state being hidden in the framework, the actual failure time is inaccessible for comparison in this case.

Next, the proposed method is compared with the conventional moving average filter method [11], where the noise degradation measurements are filtered directly using the average smoothing in the data preprocessing stage. For the moving average filter, the filter length is determined as 5 to remove the noise for the monotonic health state changes as well as retain the original degradation information as much as possible. Next, the filtered CM signals are directly applied to the degradation model in (2) and then characterizing the model with the parameter estimation method in [39]. As a result, the model parameters are estimated as $a = 0.03430$, $b = 0.8400$, $\kappa = 53465.90$, $\lambda = 7.2341$.

Table III: RUL prediction at multiple CM time instants (unit is cycle)

Monitoring Time	RUL Prediction	95% CI
250	6461	[2463, 12021]
1750	6155	[2359, 11249]
3250	5213	[1774, 9811]
4500	4149	[1134, 8253]
4750	1924	[195, 4889]
5500	977	[57, 2936]
6500	346	[17, 1641]
7250	180	[16, 1077]

By using device #13 as an illustration, the health state prediction performance in terms of the moving average filter and the proposed method are shown in Fig. 16(a) and Fig. 16(b), respectively. Considering the low noise level ($\sigma^2 = 7.3809 \times 10^{-8}$), a better health state estimation should be able to track the noisy $\Delta R_{\text{DS(on)}}$ closely and retain its monotonic increasing trend as well. Moreover, a superior 95% CI prediction of the monotonic health state is expected to follow the trend of the noisy $\Delta R_{\text{DS(on)}}$ closely and cover the noisy signals evenly.

On the one hand, in Fig. 16(a), the characterization of the degradation behavior is worse than that in Fig. 16(b), since the monotonic health state estimation (red asterisk line) based on the moving average filter cannot track the noisy $\Delta R_{\text{DS(on)}}$ accurately. At CM time instants 1750 cycles and 4500 cycles in Fig. 16(a), the predicted 95% CI of the degradation level is not well aligned with the future trend of $\Delta R_{\text{DS(on)}}$ and a portion of $\Delta R_{\text{DS(on)}}$ signals is beyond the boundaries of the predicted area. Although the predicted 95% CI is relatively narrower, the characterization of the degradation behavior is worse. The reason is that the removed noise by using the average smoothing excessively reduces the useful uncertain information. This limitation is significantly mitigated by using the proposed method, as shown in Fig. 16(b), indicating a better uncertainty management capability.

On the other hand, in Fig. 16(a), the rapid changes of the degradation behavior at CM time instant 8750 cycles cannot be well characterized, suggesting the limited model dynamics. The reason is that the moving average filter removes the noise blindly with less consideration of the internal degradation dynamics. Fig. 16(b) shows that the future degradation measurements can be tracked and covered closely with the proposed method.

Subsequently, to evaluate the health state prediction performance quantitatively, an effectiveness measure Q is defined as

$$Q = \frac{\sum_{i=1}^{13} \sum_{j=1}^{n_i} b_{i,j}}{\sum_{i=1}^{13} \sum_{j=1}^{n_i} a_{i,j}}, \tag{17}$$

where $a_{i,j}$ is the number of prediction points for the rest degradation sequence when evaluating at CM time instant $t_{i,j}$, and $b_{i,j}$ is the number of the prediction points that are within the 95% CI. As a result, the effectiveness measure Q for the

This article has been accepted for publication in a future issue of this journal, but has not been fully edited. Content may change prior to final publication. Citation information: DOI 10.1109/TIM.2021.3054429, IEEE Transactions on Instrumentation and Measurement

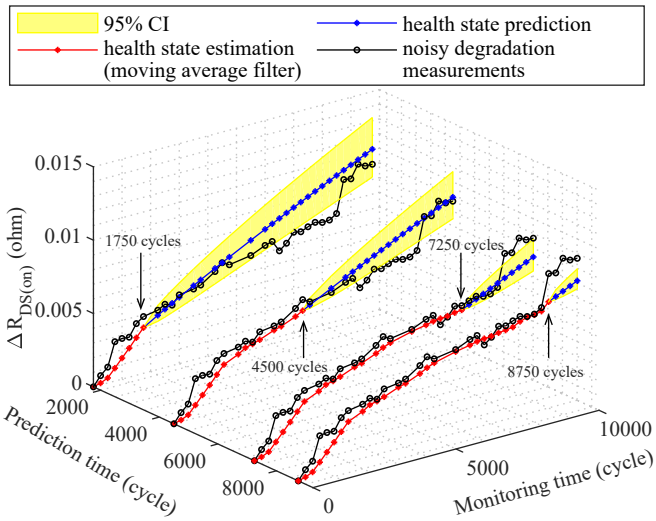

(a) Health state prediction based on the data processed with the moving average filter and the degradation model in (2).

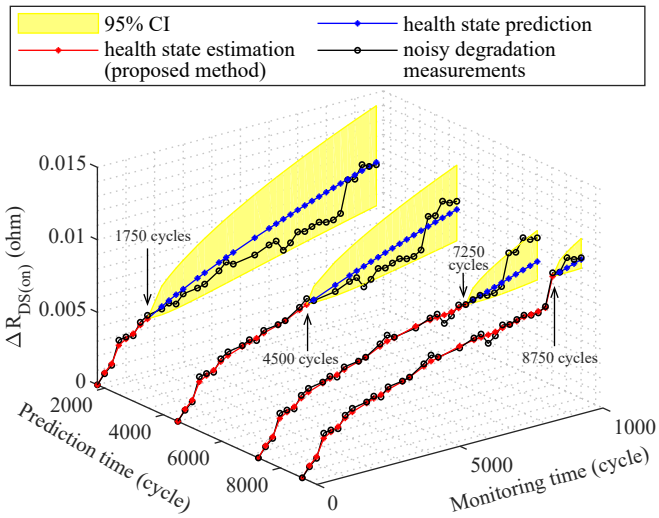

(b) Health state prediction based on the original noisy and aperiodic measurements and the proposed method.

Fig. 16. Prediction performance comparisons of the health state for device #13.

proposed method and the method based on moving averaging filter is calculated as 0.9405, 0.6798, respectively. There is a significant improvement with the proposed method for the health state prediction.

C. Discussions

Note that the case study on SiC MOSFETs aims to provide an exemplary application for industrial cases in the presence of noisy and aperiodic CM signals, which is common in the condition monitoring of power electronic systems. The proposed method is generic and can be extended to other crucial power devices or systems.

Another perspective application of the proposed framework is the implementation of high-precision CM with cost-efficient sensors. Typically, the high-precision CM signal can only be obtained by high-precision and noise-immunity sensors. However, such advanced sensors are mostly expensive and increase the system cost significantly. It is necessary to develop a method facilitating the high-precision CM with low-cost sensors. It can be facilitated with the proposed method. Firstly, the high-precision CM signals and the low-precision ones in terms of the device degradation are simultaneously acquired in the laboratory for the benchmark. With the proposed method, the high-precision CM signals can be considered as health state $x(t)$ in (3), which is latent and unobservable. The low-precision CM signal can be treated as the noisy degradation measurements $y(t)$. With the proposed method, the relationship between the high-precision CM signal $x(t)$ and the low-precision $y(t)$ in terms of the power device degradation can be explicitly developed and calibrated. Secondly, the low-precision sensor, which is usually economic, can be applied to field applications for continuous CM. With the calibrated model, the high-precision CM signal can be inferred using the low-precision one. As a result, the high-precision CM can be facilitated with economic sensors for field applications in a cost-efficient way. Similarly, other functional information of interest that is unobservable, inaccessible, or challenging to measure, can be estimated by extending (3) with a specific functional form as $y(t) = f(x(t)) + \varepsilon$.

V. Conclusions

This paper presents a method for the health state estimation and remaining useful life prediction of power devices in the presence of the noisy and aperiodic condition monitoring signals. A Gamma state-space model is applied to the degradation modeling of power devices. Three-source uncertainties that affect the evaluation accuracy, including the temporal uncertainty, measurement uncertainty, and device-to-device heterogeneity, are considered simultaneously in the framework. The numerical study indicates that the accuracy of the health assessment and remaining useful life prediction is high, and it is robust under various noise levels. The method has been implemented and verified on the SiC MOSFETs degradation dataset. It is found that the health state of SiC MOSFETs can be estimated and tracked accurately, and highly accurate predictions of the remaining useful life can be obtained.

Appendix

A1. Derivation details of the PDF of the health state $x(t)$ in (4):

$$
\begin{aligned}
f(x(t)) &= \int_0^\infty f(x(t);\nu(t),\xi^{-1}) \cdot f(\xi;\kappa,\lambda^{-1}) d\xi \\
&= \int_0^\infty \left(\frac{\xi}{\Gamma(\nu(t))} (\xi x(t))^{\nu(t)-1} \exp(-\xi x(t)) \right. \\
&\quad \left. \cdot \frac{\lambda}{\Gamma(\kappa)} (\lambda\xi)^{\kappa-1} \exp(-\lambda\xi) d\xi \right) \\
&= \frac{x(t)^{\nu(t)-1}\lambda^\kappa}{\Gamma(\nu(t))\Gamma(\kappa)(x(t)+\lambda)^{\nu(t)+\kappa-1}} \\
&\quad \cdot \int_0^\infty ((x(t)+\lambda)\xi)^{\nu(t)+\kappa-1} \exp(-(x(t)+\lambda)\xi) d\xi \\
&= \frac{x(t)^{\nu(t)-1}\lambda^\kappa \Gamma(\nu(t)+\kappa)}{\Gamma(\nu(t))\Gamma(\kappa)(x(t)+\lambda)^{\nu(t)+\kappa}}
\end{aligned}
$$

This article has been accepted for publication in a future issue of this journal, but has not been fully edited. Content may change prior to final publication. Citation information: DOI 10.1109/TIM.2021.3054429, IEEE Transactions on Instrumentation and Measurement

$$= \frac{\lambda^{\kappa} x(t)^{\nu(t)-1}}{B(\nu(t),\kappa)\cdot(x(t)+\lambda)^{\nu(t)+\kappa}}.$$

A2. Derivation details of conditional PDF of $\Delta x(t)$ given the current health state $x(t)$ in (6):

$$\begin{aligned}
f(\Delta x(t) \mid x(t)) &= \frac{f(\Delta x(t), x(t))}{f(x(t))} \\
&= \frac{\left(\begin{array}{l}\int_0^{\infty} f(\Delta x(t);\Delta\nu(t),\xi^{-1})\cdot f(x(t);\nu(t),\xi^{-1}) \\ \cdot f(\xi;\kappa,\lambda^{-1})d\xi\end{array}\right)}{\int_0^{\infty} f(x(t);\nu(t),\xi^{-1})\cdot f(\xi;\kappa,\lambda^{-1})d\xi} \\
&= \frac{\left\{\frac{\lambda^{\kappa}\Gamma(\kappa+\nu(t)+\Delta\nu(t))}{\Gamma(\kappa)\Gamma(\nu(t))\Gamma(\Delta\nu(t))}\cdot\frac{\Delta x(t)^{\Delta\nu(t)-1}x(t)^{\nu(t)-1}}{(\lambda+x(t)+\Delta x(t))^{\kappa+\nu(t)+\Delta\nu(t)}}\right\}}{\left\{\frac{x(t)^{\nu(t)-1}\lambda^{\kappa}\Gamma(\nu(t)+\kappa)}{\Gamma(\nu(t))\Gamma(\kappa)(x(t)+\lambda)^{\nu(t)+\kappa-1}}\right\}} \\
&= \frac{\Gamma(\kappa+\nu(t)+\Delta\nu(t))(\Delta x(t))^{\Delta\nu(t)-1}(x(t)+\lambda)^{\nu(t)+\kappa}}{\Gamma(\nu(t)+\kappa)\Gamma(\Delta\nu(t))(x(t)+\Delta x(t)+\lambda)^{\nu(t)+\Delta\nu(t)+\kappa}} \\
&= \frac{(\Delta x(t))^{\Delta\nu(t)-1}(x(t)+\lambda)^{\nu(t)+\kappa}}{B(\nu(t)+\kappa,\Delta\nu(t))(x(t)+\Delta x(t)+\lambda)^{\nu(t)+\Delta\nu(t)+\kappa}}.
\end{aligned}$$

A3. Proof of Corollary 1: Note that $\zeta = \frac{\nu(t)+\kappa}{\Delta\nu(t)}\cdot\frac{\Delta x(t)}{x(t)+\lambda}$. Thus, the increment $\Delta x(t)$ could be expressed as $\Delta x(t) = \frac{\Delta\nu(t)(x(t)+\lambda)}{\nu(t)+\kappa}\zeta$. Considering (6), the PDF of ζ could be developed as

$$\begin{aligned}
&f(\zeta \mid x(t)) \\
&= f(\frac{\Delta\nu(t)(x(t)+\lambda)}{\nu(t)+\kappa}\zeta \mid x(t))\cdot(\frac{\Delta\nu(t)(x(t)+\lambda)}{\nu(t)+\kappa}\zeta)' \\
&= \frac{(\frac{\Delta\nu(t)(x(t)+\lambda)}{\nu(t)+\kappa}\zeta)^{\Delta\nu(t)-1}(x(t)+\lambda)^{\nu(t)+\kappa}\cdot\frac{\Delta\nu(t)(x(t)+\lambda)}{\nu(t)+\kappa}}{B(\nu(t)+\kappa,\Delta\nu(t))(x(t)+\frac{\Delta\nu(t)(x(t)+\lambda)}{\nu(t)+\kappa}\zeta+\lambda)^{\nu(t)+\Delta\nu(t)+\kappa}} \\
&= \frac{\left(\begin{array}{l}(\nu(t)+\kappa)^{\nu(t)+\kappa}(x(t)+\lambda)^{\nu(t)+\Delta\nu(t)+\kappa} \\ \cdot(\Delta\nu(t)\zeta)^{\Delta\nu(t)-1}\Delta\nu(t)\end{array}\right)}{\left(\begin{array}{l}B(\nu(t)+\kappa,\Delta\nu(t))(x(t)+\lambda)^{\nu(t)+\Delta\nu(t)+\kappa} \\ \cdot(\nu(t)+\kappa+\Delta\nu(t)\zeta)^{\nu(t)+\kappa+\Delta\nu(t)}\end{array}\right)} \\
&= \frac{\Delta\nu(t)^{\Delta\nu(t)}(\nu(t)+\kappa)^{\nu(t)+\kappa}\zeta^{\Delta\nu(t)-1}}{B(\nu(t)+\kappa,\Delta\nu(t))(\nu(t)+\kappa+\Delta\nu(t)\zeta)^{\nu(t)+\kappa+\Delta\nu(t)}} \\
&= \frac{(2\Delta\nu(t))^{\Delta\nu(t)}(2\nu(t)+2\kappa)^{\nu(t)+\kappa}\zeta^{\Delta\nu(t)-1}}{B(\nu(t)+\kappa,\Delta\nu(t))(2\nu(t)+2\kappa+2\Delta\nu(t)\zeta)^{\nu(t)+\kappa+\Delta\nu(t)}}.
\end{aligned}$$

Thus, conditioned on the current health state $x(t)$, $\zeta \sim \mathcal{F}_{2\Delta\nu(t),2\nu(t)+2\kappa}$, and this completes the proof.

A4. Derivation details of the first part of the expectation of the log-likelihood function in (11):

$$\begin{aligned}
E\left[\log(\prod_{i=1}^{m} f(x_{i,1:n_i} \mid \boldsymbol{\Theta}_1))\right] &= \sum_{i=1}^{m} E\left[\log(f(x_{i,1:n_i} \mid \boldsymbol{\Theta}_1))\right] \\
&= \sum_{i=1}^{m} E\left[\log(f(\Delta x_{i,1},\cdots,\Delta x_{i,n_i} \mid \boldsymbol{\Theta}_1))\right] \\
&= \sum_{i=1}^{m} E\left[\log\left(\frac{\lambda^{\kappa}\Gamma(\kappa+\nu_{i,n_i})}{\Gamma(\kappa)\prod_{j=1}^{n_i}\Gamma(\Delta\nu_{i,j})}\cdot\frac{\prod_{j=1}^{n_i}\Delta x_{i,j}^{\Delta\nu_{i,j}-1}}{(\lambda+x_{i,n_i})^{\kappa+\nu_{i,n_i}}}\right)\right] \\
&= \sum_{i=1}^{m}\left(\begin{array}{l}\kappa\log\lambda+\log\Gamma(\kappa+\nu_{i,n_i})-\log\Gamma(\kappa) \\ -\sum_{j=1}^{n_i}\log\Gamma(\Delta\nu_{i,j})+\sum_{j=1}^{n_i}(\Delta\nu_{i,j}-1)E\left[\log\Delta x_{i,j}\right] \\ -(\kappa+\nu_{i,n_i})E\left[\log(\lambda+x_{i,n_i})\right]\end{array}\right).
\end{aligned}$$

A5. Derivation details of the second part of the expectation of the log-likelihood function in (12):

$$\begin{aligned}
&E\left[\log(\prod_{i=1}^{m} f(y_{i,1:n_i} \mid x_{i,1:n_i},\boldsymbol{\Theta}_2))\right] \\
&= E\left[\log(\prod_{i=1}^{m}\prod_{j=1}^{n_i} f(y_{i,j} \mid x_{i,j},\boldsymbol{\Theta}_2))\right] \\
&= E\left[\left(\sum_{i=1}^{m}\sum_{j=1}^{n_i}\log\left(\frac{1}{\sqrt{2\pi\sigma^2}}\exp\left(-\frac{(y_{i,j}-x_{i,j})^2}{2\sigma^2}\right)\right)\right)\right] \\
&= E\left[\sum_{i=1}^{m}\sum_{j=1}^{n_i}\left(\frac{1}{2}\log(2\pi\sigma^2)-\frac{1}{2\sigma^2}(y_{i,j}^2-2y_{i,j}x_{i,j}+x_{i,j}^2)\right)\right] \\
&= \sum_{i=1}^{m}\sum_{j=1}^{n_i}\left(\begin{array}{l}\frac{1}{2}\log(2\pi\sigma^2) \\ -\frac{1}{2\sigma^2}\left(y_{i,j}^2-2y_{i,j}E\left[x_{i,j}\right]+E\left[x_{i,j}^2\right]\right)\end{array}\right).
\end{aligned}$$

REFERENCES

[1] S. Yang, D. Xiang, A. Bryant, P. Mawby, L. Ran, and P. Tavner, "Condition monitoring for device reliability in power electronic converters: A review," *IEEE Trans. Power Electron.*, vol. 25, no. 11, pp. 2734–2752, Nov. 2010.

[2] S. Dusmez, M. Heydarzadeh, M. Nourani, and B. Akin, "Remaining useful lifetime estimation for power MOSFETs under thermal stress with RANSAC outlier removal," *IEEE Trans. Ind. Informat.*, vol. 13, pp. 1271–1279, Jun. 2017.

[3] S. Zhao, V. Makis, S. Chen, and Y. Li, "Health assessment method for electronic components subject to condition monitoring and hard failure," *IEEE Trans. Instrum. Meas.*, vol. 68, no. 1, pp. 138–150, Jan. 2019.

[4] S. Zhao, S. W. Chen, F. Yang, E. Ugur, B. Akin, H. Wang, "A composite failure precursor for condition monitoring and remaining useful life prediction of discrete power devices," *IEEE Trans. Ind. Informat.*, vol. 17, no. 1, pp. 688–698, Jan. 2021.

[5] A. Alghassi, S. Perinpanayagam, and M. Samie, "Stochastic RUL calculation enhanced with TDNN-based IGBT failure modeling," *IEEE Trans. Rel.*, vol. 65, no. 2, pp. 558–573, 2016.

[6] A. Ismail, L. Saidi, M. Sayadi, and M. Benbouzid, "Remaining useful life estimation for thermally aged power insulated gate bipolar transistors based on a modified maximum likelihood estimator," *Int. Trans. Elect. Energy Syst.*, vol. 30, no. 6, p. e12358, Feb. 2020.

[7] M. S. Haque, S. Choi, and J. Baek, "Auxiliary particle filtering-based estimation of remaining useful life of IGBT," *IEEE Trans. Ind. Electron.*, vol. 65, no. 3, pp. 2693–2703, Mar. 2018.

[8] W. Chen, L. Zhang, K. Pattipati, A. M. Bazzi, S. Joshi, and E. M. Dede, "Data-driven approach for fault prognosis of SiC MOSFETs," *IEEE Trans. Power Electron.*, vol. 35, no. 4, pp. 4048–4062, Aug. 2020.

[9] S. H. Ali, M. Heydarzadeh, S. Dusmez, X. Li, A. S. Kamath, and B. Akin, "Lifetime estimation of discrete IGBT devices based on gaussian process," *IEEE Trans. Ind. Appl.*, vol. 54, no. 1, pp. 395–403, Jan.-Feb. 2018.

[10] A. Ismail, L. Saidi, M. Sayadi, and M. Benbouzid, "Remaining useful lifetime prediction of thermally aged power insulated gate bipolar transistor based on gaussian process regression," *Trans. Inst. Measurement Control*, vol. 42, no. 13, pp. 2507–2518, Jun. 2020.

[11] A. Alghassi, S. Perinpanayagam, M. Samie, and T. Sreenuch, "Computationally efficient, real-time, and embeddable prognostic techniques for power electronics," *IEEE Trans. Power Electron.*, vol. 30, no. 5, pp. 2623–2634, May 2015.

[12] H. Chaoui and H. Gualous, "Online lifetime estimation of supercapacitors," *IEEE Trans. Power Electron.*, vol. 32, no. 9, pp. 7199–7206, Sep. 2017.

[13] Z. Pan and N. Balakrishnan, "Reliability modeling of degradation of products with multiple performance characteristics based on gamma processes," *Rel. Eng. & System Safety*, vol. 96, no. 8, pp. 949–957, Aug. 2011.

[14] J. Son, S. Zhou, C. Sankavaram, X. Du, and Y. Zhang, "Remaining useful life prediction based on noisy condition monitoring signals using constrained kalman filter," *Rel. Eng. & System Safety*, vol. 152, pp. 38–50, Aug. 2016.

[15] K. Le Son, M. Fouladirad, and A. Barros, "Remaining useful lifetime estimation and noisy gamma deterioration process," *Rel. Eng. & System Safety*, vol. 149, pp. 76–87, May 2016.

[16] J. R. Celaya, A. Saxena, S. Saha, and K. Goebel, "Prognostics of power MOSFETs under thermal stress accelerated aging using data-driven and model-based methodologies," in *Ann. Conf. Prognostics Health Manage. Soc.*, Montreal, QC, Sep. 2011, pp. 1–10.

[17] Q. Qin, S. Zhao, S. W. Chen, D. S. Huang, J. Liang, "Adaptive and robust prediction for the remaining useful life of electrolytic capacitors," *Microelectronics Rel.*, vol. 87, pp. 64–74, Aug. 2018.

[18] B. E. Olivares, M. A. Cerda Munoz, M. E. Orchard, and J. F. Silva, "Particle-filtering-based prognosis framework for energy storage devices with a statistical characterization of state-of-health regeneration phenomena," *IEEE Trans. Instrum. Meas.*, vol. 62, no. 2, pp. 364–376, Feb. 2013.

[19] P. Lall and H. Zhang, "Assessment of lumen degradation and remaining life of light-emitting diodes using physics-based indicators and particle filter," *J. Electron. Packaging*, vol. 137, no. 0210022, Jun. 2015.

[20] D. Wang, F. Yang, K.-L. Tsui, Q. Zhou, and S. J. Bae, "Remaining useful life prediction of lithium-ion batteries based on spherical cubature particle filter," *IEEE Trans. Instrum. Meas.*, vol. 65, no. 6, pp. 1282–1291, Jun. 2016.

[21] H.-C. Yan, J.-H. Zhou, and C. K. Pang, "Gamma process with recursive MLE for wear PDF prediction in precognitive maintenance under aperiodic monitoring," *Mechatronics*, vol. 31, pp. 68–77, Oct. 2015.

[22] X. Si, W. Wang, C. Hu, and D. Zhou, "Estimating remaining useful life with three-source variability in degradation modeling," *IEEE Trans. Rel.*, vol. 63, no. 1, pp. 167–190, Mar. 2014.

[23] Y. G. Lei, N. P. Li, J. Lin, "A new method based on stochastic process models for machine remaining useful life prediction," *IEEE Trans. Instrum. Meas.*, vol. 65, no. 12, pp. 2671–2684, Dec. 2016.

[24] M. D. Pandey, X. X. Yuan, and J. M. van Noortwijk, "The influence of temporal uncertainty of deterioration on life-cycle management of structures," *Structure Infrastructure Eng.*, vol. 5, no. 2, pp. 145–156, Jan. 2009.

[25] Q. Zhou, J. Son, S. Zhou, X. Mao, and M. Salman, "Remaining useful life prediction of individual units subject to hard failure," *IIE Trans.*, vol. 46, no. 10, pp. 1017–1030, Jun. 2014.

[26] X. Wang, P. Jiang, B. Guo, and Z. Cheng, "Real-time reliability evaluation with a general wiener process-based degradation model," *Quality Rel. Eng. Int.*, vol. 30, no. 2, pp. 205–220, Jan. 2014.

[27] Z. Zhang, X. Si, C. Hu, and X. Kong, "Degradation modeling-based remaining useful life estimation: A review on approaches for systems with heterogeneity," *Proc. Institution Mech. Engineers, Part O: J. Risk Rel.*, vol. 229, no. 4, pp. 343–355, Apr. 2015.

[28] Y. Zhou, Y. Sun, J. Mathew, R. Wolff, and L. Ma, "Latent degradation indicators estimation and prediction: A Monte Carlo approach," *Mech. Syst. Signal Process.*, vol. 25, no. 1, pp. 222–236, Jan. 2011.

[29] J. Lawless and M. Crowder, "Covariates and random effects in a gamma process model with application to degradation and failure," *Lifetime Data Analysis*, vol. 10, no. 3, pp. 213–227, Sep. 2004.

[30] J. M. van Noortwijk, "A survey of the application of gamma processes in maintenance," *Rel. Eng. & System Safety*, vol. 94, no. 1, pp. 2–21, Jan. 2009.

[31] T. Santini, S. Morand, M. Fouladirad, L. V. Phung, F. Miller, B. Foucher, A. Grall, and B. Allard, "Accelerated degradation data of SiC MOSFETs for lifetime and remaining useful life assessment," *Microelectronics Rel.*, vol. 54, no. 9-10, pp. 1718–1723, Oct. 2014.

[32] M. S. Arulampalam, S. Maskell, N. Gordon, and T. Clapp, "A tutorial on particle filters for online nonlinear/non-gaussian bayesian tracking," *IEEE Trans. Signal Process.*, vol. 50, no. 2, pp. 174–188, Feb. 2002.

[33] R. Van Der Merwe, A. Doucet, N. De Freitas, and E. A. Wan, "The unscented particle filter," in *Advances in neural inform. process. syst.*, 2001, pp. 584–590.

[34] S. J. Godsill, A. Doucet, and M. West, "Monte Carlo smoothing for nonlinear time series," *J. Amer. Statistical Assoc.*, vol. 99, no. 465, pp. 156–168, Jan. 2004.

[35] A. Khaleghei and V. Makis, "Reliability estimation of a system subject to condition monitoring with two dependent failure modes," *IIE Trans.*, vol. 48, no. 11, pp. 1058–1071, May 2016.

[36] X.-S. Si, W. Wang, C.-H. Hu, D.-H. Zhou, and M. G. Pecht, "Remaining useful life estimation based on a nonlinear diffusion degradation process," *IEEE Trans. Rel.*, vol. 61, no. 1, pp. 50–67, Mar. 2012.

[37] E. Ugur, F. Yang, S. Pu, S. Zhao, and B. Akin, "Degradation assessment and precursor identification for SiC MOSFETs under high temp cycling," *IEEE Trans. Ind. Appl.*, vol. 55, no. 3, pp. 2858–2867, Jun. 2019.

[38] F. Yang, E. Ugur, B. Akin, and G. Wang, "Design methodology of DC power cycling test setup for SiC MOSFETs," *IEEE Trans. Emerg. Sel. Topics Power Electron.*, 2019, Early access.

[39] S. Zhao, S. Chen, and H. Wang, "Degradation modeling for reliability estimation of DC film capacitors subject to humidity acceleration," *Microelectronics Rel.*, vol. 100-101, p. 113401, Sep. 2019.

Shuai Zhao (S'14-M'18) received the B.E. (Hons), M.E., and Ph.D. degrees in information and communication engineering from Northwestern Polytechnical University, Xi'an, China, in 2011, 2014, and 2018, respectively. He is currently a postdoctoral researcher with the Center of Reliable Power Electronics (CORPE), Department of Energy Technology, Aalborg University, Denmark.

From Sep. 2014 to Sep. 2016, he was a visiting Ph.D. Student with the Department of Mechanical and Industrial Engineering at the University of Toronto, Toronto, ON, Canada, with the scholarship from China Scholarship Council (CSC). In August 2018, he was a visiting scholar with the Power Electronics and Drives Laboratory, Department of Electrical and Computer Science at the University of Texas at Dallas, Richardson, TX, USA. His research interests include system informatics, intelligent condition monitoring, diagnostics & prognostics, and tailored AI tools for power electronic systems.

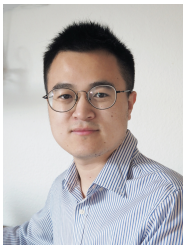

Yingzhou Peng (S'17-M'20) received the B.S. degree in electrical engineering from Harbin Engineering University, Harbin, China, in 2014, the M.S. degree in power electronics from Chongqing University, Chongqing, China, in 2017, and the Ph.D. degree in power electronics from Aalborg University, Aalborg, Denmark in 2020. He is currently working as a PosDoc with Aalborg University, Aalborg, Denmark.

He was a Visiting Researcher with the Electrical Power and Energy Conversion Lab, Cambridge University, Cambridge, U.K, in 2020. His research interests include the failure mechanisms analysis of power electronic components, the improvement of the robustness and reliability of power converters by means of condition monitoring.

Fei Yang (S'13) received the B.S. degree from Northwestern Polytechnical University, Xi'an, China, in 2011, the M.S. degree from the Center for Ultra-Wide-Area Resilient Electric Energy Transmission Networks (CURENT), the University of Tennessee, Knoxville, TN, USA, in 2017, and the Ph. D. degree from the University of Texas at Dallas, Richardson, TX, USA, in 2020, all in electrical engineering.

He is currently a System Engineer at Texas Instruments, Dallas, TX, USA. From 2012 to 2014, he was working as a researcher at Kettering University, Flint, MI, USA. His research interests include wide bandgap semiconductor device's reliability and application, power module packaging and integration, and motor drive system design.

Dr. Yang received the 2019 Mary and Richard Templeton Fellowship from the University of Texas at Dallas

Enes Ugur (S'11) received the B.Sc. degree in electrical engineering from Istanbul Technical University, Istanbul, Turkey, in 2008 and the M.Sc. degree from Yildiz Technical University, Istanbul, in 2011. He received the Ph.D. degree in Electrical Engineering from The University of Texas at Dallas, Richardson, TX, USA, in 2019. He is currently working as a power electronics systems engineer at Wolfspeed, NC, USA. His research interests include power converters and inverters, wide-bandgap devices and applications.

Bilal Akin (M'08-SM'13) received the Ph.D. degree in electrical engineering from the Texas A&M University, College Station, TX, USA, in 2007.

He was an R&D Engineer with Toshiba Industrial Division, Houston, TX, USA, from 2005 to 2008. From 2008 to 2012, he worked as an R&D Engineer at C2000 DSP Systems, Texas Instruments Incorporated. Since 2012, he has been with University of Texas at Dallas as faculty. Dr. Akin is recipient of NSF CAREER'15 award, IEEE IAS Transactions 1st Place Prize Paper Award and Top Editors Recognition Award from IEEE TVT Society, Jonsson School Faculty Research Award and Jonsson School Faculty Teaching Award. He is an Associate Editor of IEEE Transactions on Industry Applications and IEEE Transactions on Vehicular Technology. His research interests include design, control and diagnosis of electric motors & drives, digital power control and management, fault diagnosis & condition monitoring of power electronics components and ac motors.

Huai Wang (M'12-SM'17) received the B.E. degree in electrical engineering, from Huazhong University of Science and Technology, Wuhan, China, in 2007 and the Ph.D. degree in power electronics, from the City University of Hong Kong, Hong Kong, in 2012. He is currently Professor with the Center of Reliable Power Electronics (CORPE), Department of Energy Technology at Aalborg University, Denmark. He was a Visiting Scientist with the ETH Zurich, Switzerland, from Aug. to Sep. 2014, and with the Massachusetts Institute of Technology (MIT), USA, from Sep. to Nov. 2013. He was with the ABB Corporate Research Center, Switzerland, in 2009. His research addresses the fundamental challenges in modelling and validation of power electronic component failure mechanisms, and application issues in system-level predictability, condition monitoring, circuit architecture, and robustness design. He leads a project on Light AI for Cognitive Power Electronics.

Dr. Wang received the Richard M. Bass Outstanding Young Power Electronics Engineer Award from the IEEE Power Electronics Society in 2016, and the Green Talents Award from the German Federal Ministry of Education and Research in 2014. He is currently the Chair of IEEE PELS/IAS/IES Chapter in Denmark. He serves as an Associate Editor of IET Electronics Letters, IEEE JOURNAL OF EMERGING AND SELECTED TOPICS IN POWER ELECTRONICS, and IEEE TRANSACTIONS ON POWER ELECTRONICS.